Monthly Notices of the ROYAL ASTRONOMICAL SOCIETY

MNRAS **518,** 332–352 (2023) https://doi.org/10.1093/mnras/stac3129
Advance Access publication 2022 November 4

Opacity calculations in four to nine times ionized Pr, Nd, and Pm atoms for the spectral analysis of kilonovae

H. Carvajal Gallego,[1] J. Deprince,[1,2] J. C. Berengut,[3] P. Palmeri [1] and P. Quinet [1,4]★

[1] *Physique Atomique et Astrophysique, Université de Mons, B-7000 Mons, Belgium*
[2] *Institut d'Astronomie et d'Astrophysique, Université Libre de Bruxelles, B-1050 Brussels, Belgium*
[3] *School of Physics, University of New South Wales, Sydney NSW 2052, Australia*
[4] *IPNAS, Université de Liège, Sart Tilman, B-4000 Liège, Belgium*

Accepted 2022 October 25. Received 2022 October 25; in original form 2022 September 1

ABSTRACT

New atomic data for radiative transitions in Pr V–X, Nd V–X, and Pm V–X were determined by means of large-scale calculations involving three independent theoretical methods, i.e. the pseudo-relativistic Hartree–Fock method including core-polarization corrections (HFR+CPOL), the multiconfiguration Dirac–Hartree–Fock (MCDHF) method, and the configuration interaction many-body perturbation theory (CI + MBPT) implemented in the AMBIT program. This multiplatform approach allowed us to estimate the reliability of the results obtained and to extract a large amount of energy levels, wavelengths, transition probabilities, and oscillator strengths for the determination of opacities required for the analysis of the spectra emitted in the early phases of kilonovae following neutron star mergers, i.e. for typical conditions corresponding to temperatures $T > 20\,000$ K, a density $\rho = 10^{-10}$ g cm^{-3}, and a time after the merger $t = 0.1$ d. Our radiative parameters were compared in detail with the few experimental data published so far and their impact on the calculated opacities, in terms of atomic computation strategy, was also examined.

Key words: atomic data – atomic processes – opacity – neutron star mergers.

1 INTRODUCTION

Very recently, we have started a systematic investigation of spectroscopic properties for lanthanide ions in charge states between 4+ and 9+. The first two studies concerned the La V-X and Ce V-X ions (Carvajal Gallego et al. 2022a, Carvajal Gallego et al.2022b). In these works, the radiative parameters (wavelengths, transition probabilities, oscillator strengths) were determined for a very large amount of spectral lines and used for the calculation of the corresponding opacities in the astrophysical context of kilonovae.

The latter, resulting from the coalescence of neutron stars, such as the GW170817 event detected on 2017 August 17 (Abbott et al. 2017a, b), have indeed a spectrum characterized by the presence of many lines belonging to heavy elements of the periodic table among which the lanthanides play a particular role since, because of the great richness of their spectra, they contribute strongly to the observed opacities (Kasen et al. 2017). In order to estimate these opacities, it is essential to know the radiative data relating to the very numerous lines belonging to the lanthanide atoms in different ionization degrees. However, if efforts in this direction have already been made concerning the first ionization states (typically between I and IV) during the last years (see Gaigalas et al. 2019, 2020; Radžiūtė et al. 2020, 2021; Tanaka et al. 2020; Carvajal Gallego, Palmeri & Quinet 2021; Rynkun et al. 2022), there is no doubt that atomic data for the higher charge states are sorely lacking, the vast majority of spectra for lanthanide atoms more than three times ionized being completely unknown according to the NIST bibliographic database (Kramida et al. 2022). Let us just note that Banerjee et al. (2022) recently reported the first atomic opacity calculations for three lanthanide elements (Nd, Sm, and Eu) up to the ionization XI and studied their impact on the early kilonova emission.

The main purpose of the present work is to complement the recent studies we have undertaken in the case of La V–X and Ce V–X ions (Carvajal Gallego et al. 2022a, b) by calculating new radiative data for spectral lines of Pr V–X, Nd V–X, and Pm V–X ions and to deduce the corresponding opacities affecting the kilonova spectra. To do this, the same multiplatform approach as the one described in our two previous papers mentioned above was used. This approach, based on the implementation of three independent theoretical methods of atomic calculations, i.e. the relativistic Hartree–Fock method with core-polarization effects (HFR+CPOL), the multiconfiguration Dirac–Hartree–Fock (MCDHF) technique and the configuration interaction many-body perturbation theory (CI + MBPT) coded in the AMBIT program, allows to estimate the accuracy of the obtained results and therefore to provide a reliable and consistent set of wavelengths, oscillator strengths and transition probabilities for a very large number of spectral lines necessary to calculate the opacities.

2 AVAILABLE ATOMIC DATA

Among the ions considered in the present work, very few have been studied in the past, either experimentally or theoretically.

From an experimental point of view, spectral lines and energy levels were only reported for Pr V, Pr X, and Nd V ions. More

★ E-mail: pascal.quinet@umons.ac.be

precisely, in the case of Pr V, 12 transitions were classified in the region 840–2250 Å by Kaufman & Sugar (1967), which allowed them to establish the eight levels belonging to the $5p^64f$, $5p^65d$, $5p^66s$, $5p^66p$, and $5p^67s$ configurations. Using the Heidelberg electron beam ion trap (HD-EBIT), Bekker et al. (2019) measured optical inter-configuration lines of Pr X, finding the 5p–4f orbital crossing, and thereby determined the frequency of $5p^2\ ^3P_0 - 5p4f\ ^3G_0$ clock transition with an accuracy sufficient for quantum-logic spectroscopy at ultra-high resolution. In this latter work, 22 forbidden lines within the $5p^2$ and 5p4f configurations were observed giving rise to the experimental determination of 15 energy levels. Finally, 160 lines of Nd V were identified by Meftah et al. (2008) using vacuum ultraviolet normal incidence spectroscopy of a sliding spark source between 710 and 2240 Å. The analysis of this spectrum allowed to establish 48 energy levels belonging to the $5p^64f^2$, $5p^64f5d$, $5p^64f6s$, and $5p^64f6p$ configurations. Laboratory observation of the Nd V spectrum was then extended to shorter wavelength region down to 370 Å by Delghiche et al. (2015). Based on 304 spectral lines, this investigation led to the determination of 104 energy levels of the $5p^54f^25d$ core-excited configuration.

On the theoretical side, some calculations of radiative parameters were published for a limited number of electric dipole transitions in Pr, Nd, and Pm ions of interest. In this respect, the ions for which the greatest number of results were obtained are Pr V and Nd V. In the former case, the oscillator strengths and transition probabilities for the twelve lines experimentally observed by Kaufman & Sugar (1967) were computed by Karaçoban Usta & Dogan (2015) using the relativistic Hartree–Fock (HFR) method. The results obtained in this work were found to generally agree with the previous data computed for the same transitions by Migdalek & Baylis (1979) using the relativistic single-configuration Hartree–Fock method, by Migdalek & Wyrozumska (1987) by means of different versions of the relativistic model potential approach, by Savukov et al. (2003) using the relativistic many-body perturbation theory, and by Zilitis (2014) using the Dirac–Fock method. In the case of Nd V, the largest radiative data set was published by Meftah et al. (2008) and Delghiche et al. (2015) who implemented the HFR method to compute the transition probabilities for all the lines they observed in the laboratory. This study largely extended the previous work of Stanek & Migdalek (2004) who reported multiconfiguration Dirac–Fock oscillator strengths for only the $6s^2\ ^1S_0$–$6s6p\ ^{1,3}P_1$ transitions in Nd V. Finally, let us also mention the oscillator strength calculations performed on the one hand by Glushkov (1992) and Zilitis (2014) using the relativistic model potential and the Dirac–Fock method, respectively, for some resonance transitions involving low-lying configurations along the Cs isoelectronic sequence, including Pr V, Nd VI, and Pm VII, and on the other hand, those carried out by Cheng & Froese Fischer (1983) using term-dependent Hartree–Fock technique for the $4d^{10} - 4d^9nf\ ^1P$ transitions in Xe-like ions, including Pr VI and Nd VII.

3 COMPUTATION OF THE ATOMIC PARAMETERS

3.1 HFR + CPOL method

The first theoretical approach used for modelling the atomic structures and calculating the radiative parameters in Pr V–X, Nd V–X, and Pm V–X ions was the relativistic Hartree–Fock (HFR) method of Cowan (1981) modified for taking core-polarization effects into account, giving rise to the so-called HFR + CPOL method (Quinet et al. 1999, 2002). The details of this method having been recalled in our recent paper focused on Ce V–X ions (Carvajal Gallego et al. 2022a), they will not be repeated here. We will just remind that the one-body (V_{P1}) and two-body (V_{P2}) contributions of the core-polarization model potential added in the Hartree–Fock equations depend on two parameters, i.e. the dipole polarizability of the ionic core (α_d) and the cutoff radius (r_c), and take the following forms (for an atomic system with n valence electrons),

$$V_{P1} = -\frac{1}{2}\,\alpha_d \sum_{i=1}^{n} \frac{r_i^2}{(r_i^2 + r_c^2)^3} \tag{1}$$

and

$$V_{P2} = -\alpha_d \sum_{i>j} \frac{\vec{r}_i.\vec{r}_j}{[(r_i^2 + r_c^2)(r_j^2 + r_c^2)]^{3/2}}. \tag{2}$$

For each ion considered in the present work, the HFR + CPOL physical model retained was based on a Pd-like ionic core with 46 electrons filling all the subshells up to $4d^{10}$ surrounded by k valence electrons, with k ranging from 4 to 11, depending on the total number of electrons in the atomic system. This led us to estimate the core-polarization effects with the following values for the dipole polarizability (α_d) and the cutoff radius (r_c) : $\alpha_d = 0.33\ a_0^3$, $r_c = 0.71\ a_0$ for Pr V–X ions, $\alpha_d = 0.26\ a_0^3$, $r_c = 0.68\ a_0$ for Nd V–X ions, and $\alpha_d = 0.20\ a_0^3$, $r_c = 0.66\ a_0$ for Pm V–X ions. The α_d-values were obtained by extrapolating the dipole polarizabilities reported by Fraga, Karwowski & Saxena (1976) for the first ions along the Pd isoelectronic sequence, from Pd I to La XII since there are no data available in the literature for Pr XIV, Nd XV, and Pm XVI. For the cut-off radii, we used the average values $\langle r \rangle$ of the outermost core orbital (4d), as deduced from our HFR calculations. As for the intravalence correlations, they were evaluated by the explicit introduction of a large amount of interacting configurations listed in Tables 1–3 for Pr V–X, Nd V–X, and Pm V–X ions, respectively.

Finally, the radial Slater integrals corresponding to direct electrostatic interactions (F^k), exchange electrostatic interactions (G^k), and configuration interactions (R^k) were arbitrarily scaled down by a factor 0.90 while the spin-orbit parameters (ζ_{nl}), computed by the Blume–Watson method, were kept at their *ab initio* values, as recommended by Cowan (1981). It was indeed demonstrated by the latter author that this procedure allowed to artificially take into account the effect of configurations not explicitly included in the calculations in order to reduce the discrepancies between the calculated eigenvalues of the Hamiltonian and the experimental energy levels, when they are known.

Among the ions considered in the present work, only two have experimentally measured wavelengths for electric dipole transitions, namely Pr V (Kaufman & Sugar 1967) and Nd V (Meftah et al. 2008; Delghiche et al. 2015). When comparing our HFR + CPOL values with these experimental data, we found a good overall agreement (smaller than 2 per cent in most cases), the average differences $\Delta\lambda/\lambda_{Obs}$ (with $\Delta\lambda = \lambda_{HFR+CPOL} - \lambda_{Obs}$) being found to be equal to 0.011 ± 0.042 (Pr V) and -0.012 ± 0.049 (Nd V).

It is also interesting to note that, because of the collapse of the 4f orbital for some lanthanide elements, configurations of the type $5s^25p^k$, $5s^25p^{k-1}4f$, $5s^25p^{k-2}4f^2$, $5s^25p^{k-3}4f^3$ are often strongly mixed and cross each other in the energy spectrum leading even to modifications of the fundamental configurations along isoelectronic sequences. This is illustrated in Fig. 1 where the HFR + CPOL average energies are shown for Cs-like, Xe-like, I-like and Te-like Pr, Nd, and Pm ions. This explains why the ground configurations of the ions Pr V–X, Nd V–X, and Pm V–X are difficult to identify and are, for the most part, uncertain in the NIST database (Kramida et al.

Table 1. Configurations included in the HFR + CPOL calculations for Pr V–X ions.

Pr V	Pr VI	Pr VII	Pr VIII	Pr IX	Pr X
Odd parity	Even parity	Odd parity	Even parity	Odd parity	Even parity
$5s^25p^64f$	$5s^25p^6$	$5s^25p^5$	$5s^25p^4$	$5s^25p^3$	$5s^25p^2$
$5s^25p^65f$	$5s^25p^56p$	$5s^25p^46p$	$5s^25p^36p$	$5s^25p^26p$	$5s^25p6p$
$5s^25p^66f$	$5s^25p^57p$	$5s^25p^47p$	$5s^25p^37p$	$5s^25p^27p$	$5s^25p7p$
$5s^25p^67f$	$5s^25p^58p$	$5s^25p^48p$	$5s^25p^38p$	$5s^25p^28p$	$5s^25p8p$
$5s^25p^68f$	$5s^25p^54f$	$5s^25p^44f$	$5s^25p^34f$	$5s^25p^24f$	$5s^25p4f$
$5s^25p^66p$	$5s^25p^55f$	$5s^25p^45f$	$5s^25p^35f$	$5s^25p^25f$	$5s^25p5f$
$5s^25p^67p$	$5s^25p^56f$	$5s^25p^46f$	$5s^25p^36f$	$5s^25p^26f$	$5s^25p6f$
$5s^25p^68p$	$5s^25p^57f$	$5s^25p^47f$	$5s^25p^37f$	$5s^25p^27f$	$5s^25p7f$
$5s^25p^54f^2$	$5s^25p^58f$	$5s^25p^48f$	$5s^25p^38f$	$5s^25p^28f$	$5s^25p8f$
$5s^25p^55d^2$	$5s^25p^44f^2$	$5s^25p^34f^2$	$5s^25p^24f^2$	$5s^25p4f^2$	$5s^24f^2$
$5s^25p^56s^2$	$5s^25p^45d^2$	$5s^25p^35d^2$	$5s^25p^25d^2$	$5s^25p5d^2$	$5s^25d^2$
$5s^25p^55d6s$	$5s^25p^46s^2$	$5s^25p^36s^2$	$5s^25p^26s^2$	$5s^25p6s^2$	$5s^26s^2$
$5s5p^64f5d$	$5s^25p^45d6s$	$5s^25p^35d6s$	$5s^25p^25d6s$	$5s^25p5d6s$	$5s^25d6s$
$5s5p^64f6d$	$5s5p^65d$	$5s5p^55d$	$5s5p^45d$	$5s5p^35d$	$5s5p^25d$
$5s5p^64f7d$	$5s5p^66d$	$5s5p^56d$	$5s5p^46d$	$5s5p^36d$	$5s5p^26d$
$5s5p^64f8d$	$5s5p^67d$	$5s5p^57d$	$5s5p^47d$	$5s5p^37d$	$5s5p^27d$
$5s5p^64f6s$	$5s5p^68d$	$5s5p^58d$	$5s5p^48d$	$5s5p^38d$	$5s5p^28d$
$5s5p^64f7s$	$5s5p^66s$	$5s5p^56s$	$5s5p^46s$	$5s5p^36s$	$5s5p^26s$
$5s5p^64f8s$	$5s5p^67s$	$5s5p^57s$	$5s5p^47s$	$5s5p^37s$	$5s5p^27s$
$5p^64f^3$	$5s5p^68s$	$5s5p^58s$	$5s5p^48s$	$5s5p^38s$	$5s5p^28s$
	$5s5p^54f5d$	$5s5p^44f5d$	$5s5p^34f5d$	$5s5p^24f5d$	$5s5p4f5d$
	$5s5p^54f6d$	$5s5p^44f6d$	$5s5p^34f6d$	$5s5p^24f6d$	$5s5p4f6d$
	$5s5p^54f7d$	$5s5p^44f7d$	$5s5p^34f7d$	$5s5p^24f7d$	$5s5p4f7d$
	$5s5p^54f8d$	$5s5p^44f8d$	$5s5p^34f8d$	$5s5p^24f8d$	$5s5p4f8d$
	$5s5p^54f6s$	$5s5p^44f6s$	$5s5p^34f6s$	$5s5p^24f6s$	$5s5p4f6s$
	$5s5p^54f7s$	$5s5p^44f7s$	$5s5p^34f7s$	$5s5p^24f7s$	$5s5p4f7s$
	$5s5p^54f8s$	$5s5p^44f8s$	$5s5p^34f8s$	$5s5p^24f8s$	$5s5p4f8s$
	$5p^54f^3$	$5p^44f^3$	$5p^6$	$5p^5$	$5p^4$
	$5p^64f^2$	$5p^54f^2$	$5p^44f^2$	$5p^24f^3$	$5p4f^3$
		$5p^64f$	$5p^54f$	$5p^34f^2$	$5p^24f^2$
				$5p^44f$	$5p^34f$
Even parity	Odd parity	Even parity	Odd parity	Even parity	Odd parity
$5s^25p^66s$	$5s^25p^56s$	$5s^25p^46s$	$5s^25p^36s$	$5s^25p^26s$	$5s^25p6s$
$5s^25p^67s$	$5s^25p^57s$	$5s^25p^47s$	$5s^25p^37s$	$5s^25p^27s$	$5s^25p7s$
$5s^25p^68s$	$5s^25p^58s$	$5s^25p^48s$	$5s^25p^38s$	$5s^25p^28s$	$5s^25p8s$
$5s^25p^65d$	$5s^25p^55d$	$5s^25p^45d$	$5s^25p^35d$	$5s^25p^25d$	$5s^25p5d$
$5s^25p^66d$	$5s^25p^56d$	$5s^25p^46d$	$5s^25p^36d$	$5s^25p^26d$	$5s^25p6d$
$5s^25p^67d$	$5s^25p^57d$	$5s^25p^47d$	$5s^25p^37d$	$5s^25p^27d$	$5s^25p7d$
$5s^25p^68d$	$5s^25p^58d$	$5s^25p^48d$	$5s^25p^38d$	$5s^25p^28d$	$5s^25p8d$
$5s^25p^65g$	$5s^25p^55g$	$5s^25p^45g$	$5s^25p^35g$	$5s^25p^25g$	$5s^25p5g$
$5s^25p^66g$	$5s^25p^56g$	$5s^25p^46g$	$5s^25p^36g$	$5s^25p^26g$	$5s^25p6g$
$5s^25p^67g$	$5s^25p^57g$	$5s^25p^47g$	$5s^25p^37g$	$5s^25p^27g$	$5s^25p7g$
$5s^25p^68g$	$5s^25p^58g$	$5s^25p^48g$	$5s^25p^38g$	$5s^25p^28g$	$5s^25p8g$
$5s^25p^54f5d$	$5s^25p^44f5d$	$5s^25p^34f5d$	$5s^25p^24f5d$	$5s^25p4f5d$	$5s^24f5d$
$5s^25p^54f6s$	$5s^25p^44f6s$	$5s^25p^34f6s$	$5s^25p^24f6s$	$5s^25p4f6s$	$5s^24f6s$
$5s5p^64f^2$	$5s5p^66p$	$5s5p^6$	$5s5p^5$	$5s5p^4$	$5s5p^3$
$5s5p^64f6p$	$5s5p^67p$	$5s5p^56p$	$5s5p^46p$	$5s5p^36p$	$5s5p^26p$
$5s5p^64f7p$	$5s5p^68p$	$5s5p^57p$	$5s5p^47p$	$5s5p^37p$	$5s5p^27p$
$5s5p^64f8p$	$5s5p^64f$	$5s5p^58p$	$5s5p^48p$	$5s5p^38p$	$5s5p^28p$
$5p^64f^25d$	$5s5p^65f$	$5s5p^54f$	$5s5p^44f$	$5s5p^34f$	$5s5p^24f$
	$5s5p^66f$	$5s5p^55f$	$5s5p^45f$	$5s5p^35f$	$5s5p^25f$
	$5s5p^67f$	$5s5p^56f$	$5s5p^46f$	$5s5p^36f$	$5s5p^26f$
	$5s5p^68f$	$5s5p^57f$	$5s5p^47f$	$5s5p^37f$	$5s5p^27f$
	$5s5p^54f^2$	$5s5p^58f$	$5s5p^48f$	$5s5p^38f$	$5s5p^28f$
	$5s5p^54f6p$	$5s5p^44f^2$	$5s5p^34f^2$	$5s5p^24f^2$	$5s5p4f^2$
	$5s5p^54f7p$	$5s5p^44f6p$	$5s5p^34f6p$	$5s5p^24f6p$	$5s5p4f6p$
	$5s5p^54f8p$	$5s5p^44f7p$	$5s5p^34f7p$	$5s5p^24f7p$	$5s5p4f7p$
	$5p^54f^25d$	$5s5p^44f8p$	$5s5p^34f8p$	$5s5p^24f8p$	$5s5p4f8p$
	$5p^64f5d$	$5p^65d$	$5p^55d$	$5p^45d$	$5p^35d$
		$5p^44f^25d$	$5p^44f5d$	$5p^24f^25d$	$5p4f^25d$
		$5p^54f5d$		$5p^34f5d$	$5p^24f5d$

Table 2. Configurations included in the HFR + CPOL calculations for Nd V–X ions.

Nd V	Nd VI	Nd VII	Nd VIII	Nd IX	Nd X
Even parity	Odd parity	Even parity	Odd parity	Even parity	Odd parity
$5s^25p^64f^2$	$5s^25p^64f$	$5s^25p^6$	$5s^25p^5$	$5s^25p^34f$	$5s^25p^24f$
$5s^25p^64f5f$	$5s^25p^65f$	$5s^25p^56p$	$5s^25p^46p$	$5s^25p^35f$	$5s^25p^25f$
$5s^25p^64f6f$	$5s^25p^66f$	$5s^25p^57p$	$5s^25p^47p$	$5s^25p^36f$	$5s^25p^26f$
$5s^25p^64f7f$	$5s^25p^67f$	$5s^25p^58p$	$5s^25p^48p$	$5s^25p^37f$	$5s^25p^27f$
$5s^25p^64f8f$	$5s^25p^68f$	$5s^25p^54f$	$5s^25p^44f$	$5s^25p^38f$	$5s^25p^28f$
$5s^25p^64f6p$	$5s^25p^66p$	$5s^25p^55f$	$5s^25p^45f$	$5s^25p^4$	$5s^25p^3$
$5s^25p^64f7p$	$5s^25p^67p$	$5s^25p^56f$	$5s^25p^46f$	$5s^25p^36p$	$5s^25p^26p$
$5s^25p^64f8p$	$5s^25p^68p$	$5s^25p^57f$	$5s^25p^47f$	$5s^25p^37p$	$5s^25p^27p$
$5s^25p^65d^2$	$5s^25p^54f^2$	$5s^25p^58f$	$5s^25p^48f$	$5s^25p^38p$	$5s^25p^28p$
$5s^25p^65d6d$	$5s^25p^55d^2$	$5s^25p^44f^2$	$5s^25p^34f^2$	$5s^25p^24f^2$	$5s^25p4f^2$
$5s^25p^65d7d$	$5s^25p^56s^2$	$5s^25p^45d^2$	$5s^25p^35d^2$	$5s^25p^25d^2$	$5s^25p5d^2$
$5s^25p^65d8d$	$5s^25p^55d6s$	$5s^25p^46s^2$	$5s^25p^36s^2$	$5s^25p^26s^2$	$5s^25p6s^2$
$5s^25p^66s^2$	$5s5p^64f5d$	$5s^25p^45d6s$	$5s^25p^35d6s$	$5s^25p^25d6s$	$5s^25p5d6s$
$5s^25p^65d6s$	$5s5p^64f6d$	$5s5p^65d$	$5s5p^55d$	$5s5p^45d$	$5s5p^35d$
$5s^25p^65d7s$	$5s5p^64f7d$	$5s5p^66d$	$5s5p^56d$	$5s5p^46d$	$5s5p^36d$
$5s^25p^65d8s$	$5s5p^64f8d$	$5s5p^67d$	$5s5p^57d$	$5s5p^47d$	$5s5p^37d$
$5s5p^64f^25d$	$5s5p^64f6s$	$5s5p^68d$	$5s5p^58d$	$5s5p^48d$	$5s5p^38d$
$5s5p^64f^26d$	$5s5p^64f7s$	$5s5p^66s$	$5s5p^56s$	$5s5p^46s$	$5s5p^36s$
$5s5p^64f^27d$	$5s5p^64f8s$	$5s5p^67s$	$5s5p^57s$	$5s5p^47s$	$5s5p^37s$
$5s5p^64f^28d$	$5p^64f^3$	$5s5p^68s$	$5s5p^58s$	$5s5p^48s$	$5s5p^38s$
$5s5p^64f^26s$		$5s5p^54f5d$	$5s5p^44f5d$	$5s5p^34f5d$	$5s5p^24f5d$
$5s5p^64f^27s$		$5s5p^54f6d$	$5s5p^44f6d$	$5s5p^34f6d$	$5s5p^24f6d$
$5s5p^64f^28s$		$5s5p^54f7d$	$5s5p^44f7d$	$5s5p^34f7d$	$5s5p^24f7d$
$5s^25p^54f^3$		$5s5p^54f8d$	$5s5p^44f8d$	$5s5p^34f8d$	$5s5p^24f8d$
		$5s5p^54f6s$	$5s5p^44f6s$	$5s5p^34f6s$	$5s5p^24f6s$
		$5s5p^54f7s$	$5s5p^44f7s$	$5s5p^34f7s$	$5s5p^24f7s$
		$5s5p^54f8s$	$5s5p^44f8s$	$5s5p^34f8s$	$5s5p^24f8s$
		$5p^54f^3$	$5p^44f^3$	$5p^6$	$5p^5$
		$5p^64f^2$	$5p^54f^2$	$5p^44f^2$	$5p^24f^3$
			$5p^64f$	$5p^54f$	$5p^34f^2$
					$5p^44f$
Odd parity	Even parity	Odd parity	Even parity	Odd parity	Even parity
$5s^25p^64f6s$	$5s^25p^66s$	$5s^25p^56s$	$5s^25p^46s$	$5s^25p^36s$	$5s^25p^26s$
$5s^25p^64f7s$	$5s^25p^67s$	$5s^25p^57s$	$5s^25p^47s$	$5s^25p^37s$	$5s^25p^27s$
$5s^25p^64f8s$	$5s^25p^68s$	$5s^25p^58s$	$5s^25p^48s$	$5s^25p^38s$	$5s^25p^28s$
$5s^25p^64f5d$	$5s^25p^65d$	$5s^25p^55d$	$5s^25p^45d$	$5s^25p^35d$	$5s^25p^25d$
$5s^25p^64f6d$	$5s^25p^66d$	$5s^25p^56d$	$5s^25p^46d$	$5s^25p^36d$	$5s^25p^26d$
$5s^25p^64f7d$	$5s^25p^67d$	$5s^25p^57d$	$5s^25p^47d$	$5s^25p^37d$	$5s^25p^27d$
$5s^25p^64f8d$	$5s^25p^68d$	$5s^25p^58d$	$5s^25p^48d$	$5s^25p^38d$	$5s^25p^28d$
$5s^25p^64f5g$	$5s^25p^65g$	$5s^25p^55g$	$5s^25p^45g$	$5s^25p^35g$	$5s^25p^25g$
$5s^25p^64f6g$	$5s^25p^66g$	$5s^25p^56g$	$5s^25p^46g$	$5s^25p^36g$	$5s^25p^26g$
$5s^25p^64f7g$	$5s^25p^67g$	$5s^25p^57g$	$5s^25p^47g$	$5s^25p^37g$	$5s^25p^27g$
$5s^25p^64f8g$	$5s^25p^68g$	$5s^25p^58g$	$5s^25p^48g$	$5s^25p^38g$	$5s^25p^28g$
$5s^25p^65d6p$	$5s^25p^54f5d$	$5s^25p^44f5d$	$5s^25p^34f5d$	$5s^25p^24f5d$	$5s^25p4f5d$
$5s^25p^65d7p$	$5s^25p^54f6s$	$5s^25p^44f6s$	$5s^25p^34f6s$	$5s^25p^24f6s$	$5s^25p4f6s$
$5s^25p^65d8p$	$5s5p^64f^2$	$5s5p^66p$	$5s5p^6$	$5s5p^5$	$5s5p^4$
$5s^25p^65d5f$	$5s5p^64f6p$	$5s5p^67p$	$5s5p^56p$	$5s5p^46p$	$5s5p^36p$
$5s^25p^65d6f$	$5s5p^64f7p$	$5s5p^68p$	$5s5p^57p$	$5s5p^47p$	$5s5p^37p$
$5s^25p^65d7f$	$5s5p^64f8p$	$5s5p^64f$	$5s5p^58p$	$5s5p^48p$	$5s5p^38p$
$5s^25p^65d8f$	$5p^64f^25d$	$5s5p^65f$	$5s5p^54f$	$5s5p^44f$	$5s5p^34f$
$5s^25p^54f^25d$		$5s5p^66f$	$5s5p^55f$	$5s5p^45f$	$5s5p^35f$
$5s^25p^54f^26s$		$5s5p^67f$	$5s5p^56f$	$5s5p^46f$	$5s5p^36f$
$5s^25p^55d^3$		$5s5p^68f$	$5s5p^57f$	$5s5p^47f$	$5s5p^37f$
$5s5p^64f^3$		$5s5p^54f^2$	$5s5p^58f$	$5s5p^48f$	$5s5p^38f$
$5s5p^64f^26p$		$5s5p^54f6p$	$5s5p^44f^2$	$5s5p^34f^2$	$5s5p^24f^2$
$5s5p^64f^27p$		$5s5p^54f7p$	$5s5p^44f6p$	$5s5p^34f6p$	$5s5p^24f6p$
$5s5p^64f^28p$		$5s5p^54f8p$	$5s5p^44f7p$	$5s5p^34f7p$	$5s5p^24f7p$
		$5p^54f^25d$	$5s5p^44f8p$	$5s5p^34f8p$	$5s5p^24f8p$
		$5p^64f5d$	$5p^65d$	$5p^55d$	$5p^45d$
			$5p^44f^25d$	$5p^44f5d$	$5p^24f^25d$
			$5p^54f5d$		$5p^34f5d$

Table 3. Configurations included in the HFR + CPOL calculations for Pm V–X ions.

Pm V	Pm VI	Pm VII	Pm VIII	Pm IX	Pm X
Odd parity	Even parity	Odd parity	Even parity	Odd parity	Even parity
$5s^25p^64f^3$	$5s^25p^64f^2$	$5s^25p^64f$	$5s^25p^54f$	$5s^25p^34f^2$	$5s^25p^24f^2$
$5s^25p^64f^25f$	$5s^25p^64f5f$	$5s^25p^65f$	$5s^25p^55f$	$5s^25p^35d^2$	$5s^25p^25d^2$
$5s^25p^64f^26f$	$5s^25p^64f6f$	$5s^25p^66f$	$5s^25p^56f$	$5s^25p^36s^2$	$5s^25p^26s^2$
$5s^25p^64f^27f$	$5s^25p^64f7f$	$5s^25p^67f$	$5s^25p^57f$	$5s^25p^5$	$5s^25p^34f$
$5s^25p^64f^28f$	$5s^25p^64f8f$	$5s^25p^68f$	$5s^25p^58f$	$5s^25p^46p$	$5s^25p^35f$
$5s^25p^64f^26p$	$5s^25p^64f6p$	$5s^25p^66p$	$5s^25p^6$	$5s^25p^47p$	$5s^25p^36f$
$5s^25p^64f^27p$	$5s^25p^64f7p$	$5s^25p^67p$	$5s^25p^56p$	$5s^25p^48p$	$5s^25p^37f$
$5s^25p^64f^28p$	$5s^25p^64f8p$	$5s^25p^68p$	$5s^25p^57p$	$5s^25p^44f$	$5s^25p^38f$
$5s5p^64f^35d$	$5s^25p^65d^2$	$5s^25p^54f^2$	$5s^25p^58p$	$5s^25p^45f$	$5s^25p^4$
$5s5p^64f^36d$	$5s^25p^65d6d$	$5s^25p^55d^2$	$5s^25p^44f^2$	$5s^25p^46f$	$5s^25p^36p$
$5s5p^64f^37d$	$5s^25p^65d7d$	$5s^25p^56s^2$	$5s^25p^45d^2$	$5s^25p^47f$	$5s^25p^37p$
$5s5p^64f^38d$	$5s^25p^65d8d$	$5s^25p^55d6s$	$5s^25p^46s^2$	$5s^25p^48f$	$5s^25p^38p$
$5s5p^64f^36s$	$5s^25p^66s^2$	$5s5p^64f5d$	$5s^25p^45d6s$	$5s^25p^35d6s$	$5s^25p^25d6s$
$5s5p^64f^37s$	$5s^25p^65d6s$	$5s5p^64f6d$	$5s5p^65d$	$5s5p^55d$	$5s5p^45d$
$5s5p^64f^38s$	$5s^25p^65d7s$	$5s5p^64f7d$	$5s5p^66d$	$5s5p^56d$	$5s5p^46d$
$5s^25p^65d^26p$	$5s^25p^65d8s$	$5s5p^64f8d$	$5s5p^67d$	$5s5p^57d$	$5s5p^47d$
$5s^25p^65d^27p$	$5s5p^64f^25d$	$5s5p^64f6s$	$5s5p^68d$	$5s5p^58d$	$5s5p^48d$
$5s^25p^65d^28p$	$5s5p^64f^26d$	$5s5p^64f7s$	$5s5p^66s$	$5s5p^56s$	$5s5p^46s$
$5s^25p^65d^25f$	$5s5p^64f^27d$	$5s5p^64f8s$	$5s5p^67s$	$5s5p^57s$	$5s5p^47s$
$5s^25p^65d^26f$	$5s5p^64f^28d$	$5p^64f^3$	$5s5p^68s$	$5s5p^58s$	$5s5p^48s$
$5s^25p^65d^27f$	$5s5p^64f^26s$		$5s5p^54f5d$	$5s5p^44f5d$	$5s5p^34f5d$
$5s^25p^65d^28f$	$5s5p^64f^27s$		$5s5p^54f6d$	$5s5p^44f6d$	$5s5p^34f6d$
	$5s5p^64f^28s$		$5s5p^54f7d$	$5s5p^44f7d$	$5s5p^34f7d$
	$5s^25p^54f^3$		$5s5p^54f8d$	$5s5p^44f8d$	$5s5p^34f8d$
			$5s5p^54f6s$	$5s5p^44f6s$	$5s5p^34f6s$
			$5s5p^54f7s$	$5s5p^44f7s$	$5s5p^34f7s$
			$5s5p^54f8s$	$5s5p^44f8s$	$5s5p^34f8s$
			$5p^54f^3$	$5p^44f^3$	$5p^6$
			$5p^64f^2$	$5p^54f^2$	$5p^44f^2$
				$5p^64f$	$5p^54f$
Even parity	Odd parity	Even parity	Odd parity	Even parity	Odd parity
$5s^25p^65d^3$	$5s^25p^64f6s$	$5s^25p^66s$	$5s^25p^56s$	$5s^25p^46s$	$5s^25p^36s$
$5s^25p^65d^26d$	$5s^25p^64f7s$	$5s^25p^67s$	$5s^25p^57s$	$5s^25p^47s$	$5s^25p^37s$
$5s^25p^65d^27d$	$5s^25p^64f8s$	$5s^25p^68s$	$5s^25p^58s$	$5s^25p^48s$	$5s^25p^38s$
$5s^25p^65d^28d$	$5s^25p^64f5d$	$5s^25p^65d$	$5s^25p^55d$	$5s^25p^45d$	$5s^25p^35d$
$5s^25p^65d^26s$	$5s^25p^64f6d$	$5s^25p^66d$	$5s^25p^56d$	$5s^25p^46d$	$5s^25p^36d$
$5s^25p^65d^27s$	$5s^25p^64f7d$	$5s^25p^67d$	$5s^25p^57d$	$5s^25p^47d$	$5s^25p^37d$
$5s^25p^65d^28s$	$5s^25p^64f8d$	$5s^25p^68d$	$5s^25p^58d$	$5s^25p^48d$	$5s^25p^38d$
$5s^25p^64f^26s$	$5s^25p^64f5g$	$5s^25p^65g$	$5s^25p^55g$	$5s^25p^45g$	$5s^25p^35g$
$5s^25p^64f^27s$	$5s^25p^64f6g$	$5s^25p^66g$	$5s^25p^56g$	$5s^25p^46g$	$5s^25p^36g$
$5s^25p^64f^28s$	$5s^25p^64f7g$	$5s^25p^67g$	$5s^25p^57g$	$5s^25p^47g$	$5s^25p^37g$
$5s^25p^64f^25d$	$5s^25p^64f8g$	$5s^25p^68g$	$5s^25p^58g$	$5s^25p^48g$	$5s^25p^38g$
$5s^25p^64f^26d$	$5s^25p^65d6p$	$5s^25p^54f5d$	$5s^25p^44f5d$	$5s^25p^34f5d$	$5s^25p^24f5d$
$5s^25p^64f^27d$	$5s^25p^65d7p$	$5s^25p^54f6s$	$5s^25p^44f6s$	$5s^25p^34f6s$	$5s^25p^24f6s$
$5s^25p^64f^28d$	$5s^25p^65d8p$	$5s5p^64f^2$	$5s5p^66p$	$5s5p^6$	$5s5p^5$
$5s^25p^64f^25g$	$5s^25p^65d5f$	$5s5p^64f6p$	$5s5p^67p$	$5s5p^56p$	$5s5p^46p$
$5s^25p^64f^26g$	$5s^25p^65d6f$	$5s5p^64f7p$	$5s5p^68p$	$5s5p^57p$	$5s5p^47p$
$5s^25p^64f^27g$	$5s^25p^65d7f$	$5s5p^64f8p$	$5s5p^64f$	$5s5p^58p$	$5s5p^48p$
$5s^25p^64f^28g$	$5s^25p^65d8f$	$5p^64f^25d$	$5s5p^65f$	$5s5p^54f$	$5s5p^44f$
$5s^25p^54f^35d$	$5s^25p^54f^25d$		$5s5p^66f$	$5s5p^55f$	$5s5p^45f$
$5s^25p^54f^36s$	$5s^25p^54f^26s$		$5s5p^67f$	$5s5p^56f$	$5s5p^46f$
$5s5p^64f^4$	$5s^25p^55d^3$		$5s5p^68f$	$5s5p^57f$	$5s5p^47f$
$5s5p^64f^36p$	$5s5p^64f^3$		$5s5p^54f^2$	$5s5p^58f$	$5s5p^48f$
$5s5p^64f^37p$	$5s5p^64f^26p$		$5s5p^54f6p$	$5s5p^44f^2$	$5s5p^34f^2$
$5s5p^64f^38p$	$5s5p^64f^27p$		$5s5p^54f7p$	$5s5p^44f6p$	$5s5p^34f6p$
	$5s5p^64f^28p$		$5s5p^54f8p$	$5s5p^44f7p$	$5s5p^34f7p$
			$5p^54f^25d$	$5s5p^44f8p$	$5s5p^34f8p$
			$5p^64f5d$	$5p^65d$	$5p^55d$
				$5p^44f^25d$	$5p^44f5d$
				$5p^54f5d$	

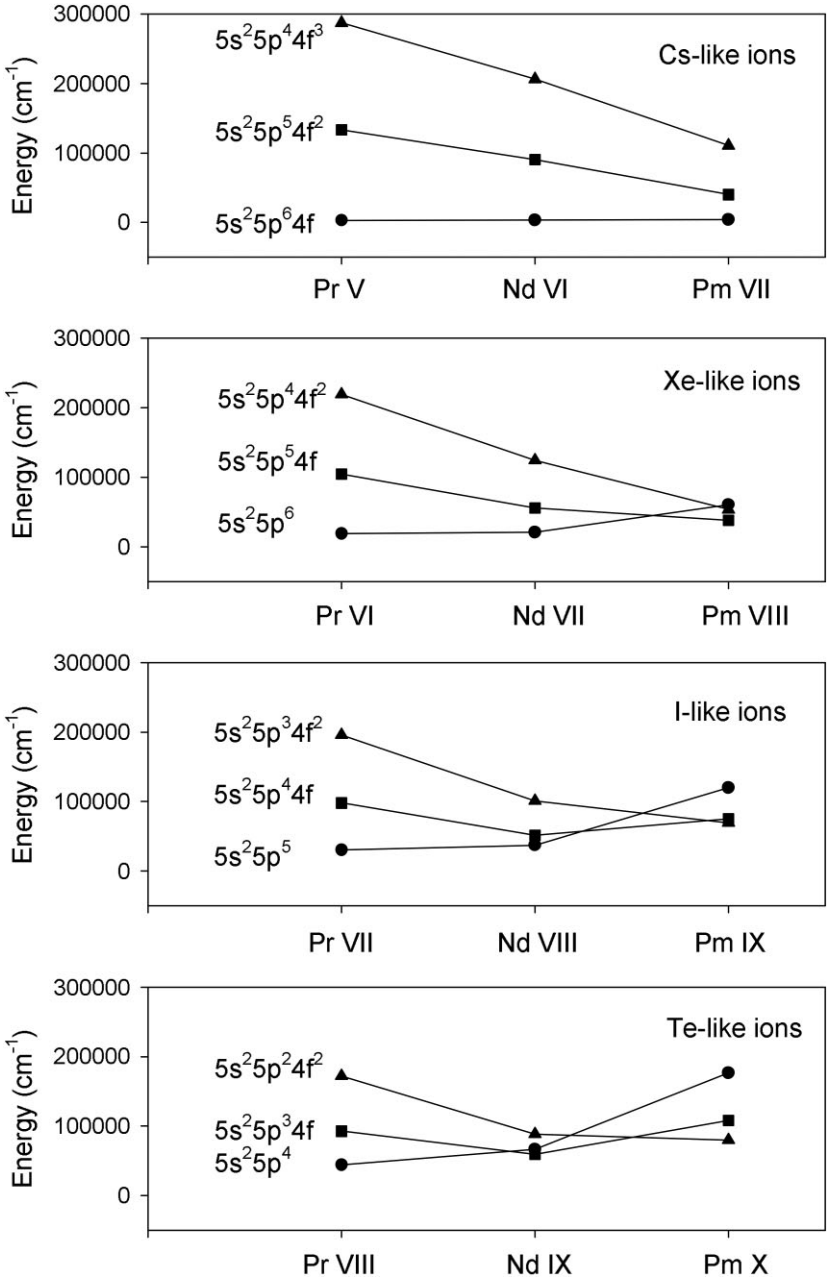

Figure 1. Calculated average energies for low-lying configurations in Cs-like, Xe-like, I-like and Te-like Pr, Nd, and Pm ions.

2022). In Table 4, we give the configuration and the *LS*-coupling spectroscopic designation of the ground level obtained in our work for each ion. If our results confirm the ground-state configurations determined by Kilbane & O'Sullivan (2010), the majority of the spectroscopic designations listed in Table 4 are new.

3.2 MCDHF method

The second computational procedure used in our work was based on the MCDHF method, as described by Grant (2007) and Froese Fischer et al. (2016), using the GRASP2018 code (Froese Fischer et al. 2019) which is the most recent version of the General Relativistic Atomic Structure Program (GRASP). The same strategy as the one developed in our previous works (Carvajal Gallego et al. 2022a, b) was followed in the present study for calculating the atomic structures and radiative parameters in a selected sample of Pr, Nd, and Pm ions, namely Pr V, Pr X, Nd V, Nd VI, Pm VI, and Pm IX. For each of these ions, valence–valence (VV) and core–valence (CV) correlations were included step by step from a list of configurations, constituting the so-called multireference (MR), among which all allowed transitions were calculated.

In the case of Pr V and Nd VI, the MR was chosen to include the $5p^6 4f$, $5p^5 4f^2$, $5p^5 5d^2$ odd- and $5p^6 5d$, $5p^5 4f 5d$ even-parity configurations. For Nd V and Pm VI, the MR consisted of $5p^6 4f^2$, $5p^6 5d^2$ even- and $5p^6 4f 5d$, $5p^5 5d^3$ odd-parity configurations. For these ions, the orbitals 1s–4f were optimized on the respective ground configurations (i.e. $5p^6 4f$ for Pr V and Nd VI and $5p^6 4f^2$ for Nd V and Pm VI) while 5d orbital was optimized using the MR configurations, keeping all other orbitals fixed. Two VV models were built by adding single and double (SD) excitations from 5s, 5p, 5d, 4f to 5s, 5p, 5d,

Table 4. Ground states of Pr V–X, Nd V–X, and Pm V–X ions.

Ion	Configuration			Level
	NIST[a]	K&O[b]	This work	This work
Pr V	$5s^25p^64f$	$5s^25p^64f$	$5s^25p^64f$	$^2F^o_{5/2}$
Pr VI	$5s^25p^6$	$5s^25p^6$	$5s^25p^6$	$^1S_0$
Pr VII	$5s^25p^44f$	$5s^25p^5$	$5s^25p^5$	$^2P^o_{3/2}$
Pr VIII	$5s^25p^34f$	$5s^25p^4$	$5s^25p^4$	$^3P_2$
Pr IX	$5s^25p^24f$	$5s^25p^3$	$5s^25p^3$	$^4S^o_{3/2}$
Pr X	$5s^24f^2$	$5s^25p^2$	$5s^25p^2$	$^3P_0$
Nd V	$5s^25p^64f^2$	$5s^25p^64f^2$	$5s^25p^64f^2$	$^3H_4$
Nd VI	$5s^25p^54f^2$	$5s^25p^64f$	$5s^25p^64f$	$^2F^o_{5/2}$
Nd VII	$5s^25p^44f^2$	$5s^25p^6$	$5s^25p^6$	$^1S_0$
Nd VIII	$5s^25p^34f^2$	$5s^25p^5$	$5s^25p^5$	$^2P^o_{3/2}$
Nd IX	$5s^25p^24f^2$	$5s^25p^34f$	$5s^25p^34f$	$^5F_3$
Nd X	$5s^25p4f^2$	$5s^25p^24f$	$5s^25p^24f$	$^4G^o_{5/2}$
Pm V	$5s^25p^64f^3$	$5s^25p^64f^3$	$5s^25p^64f^3$	$^4I^o_{9/2}$
Pm VI	$5s^25p^54f^3$	$5s^25p^64f^2$	$5s^25p^64f^2$	$^3H_4$
Pm VII	$5s^25p^44f^3$	$5s^25p^64f$	$5s^25p^64f$	$^2F^o_{5/2}$
Pm VIII	$5s^25p^34f^3$	$5s^25p^54f$	$5s^25p^54f$	$^5H_5$
Pm IX	$5s^25p^24f^3$	$5s^25p^34f^2$	$5s^25p^34f^2$	$^6H^o_{9/2}$
Pm X	$5s^25p4f^3$	$5s^25p^24f^2$	$5s^25p^24f^2$	$^5I_4$

[a]Kramida et al. (2022), also partially compiled in Martin, Zalubas & Hagan (1978).
[b] Kilbane & O'Sullivan (2010).

5f, 5g and to 6s, 6p, 6d, 6f, 5g active orbitals, for VV1 and VV2 models, respectively. From the latter, a CV model was then built by adding SD excitations from the 4d core orbital to the MR valence orbitals, namely 5s, 5p, 5d, and 4f. For Pr V and Nd VI, this gave rise to a total of 667 030 and 767 797 configuration state functions (CSFs), for the odd and even parities, respectively and for Nd V and Pm VI to 142 859 and 842 073 CSFs, for the even and odd parities, respectively.

For Pr X, the MR included the $5s^25p^2$, $5s^25p4f$, $5s^24f^2$ even- and the $5s5p^3$, $5s5p^24f$, $5s^25p5d$ odd-parity configurations. Here the orbitals 1s–5p were optimized on the $5s^25p^2$ ground configuration while the 4f and 5d orbitals were optimized using the MR configurations, keeping all other orbitals fixed. In the case of Pm IX, the MR was composed of the $5s^25p^34f^2$, $5s^25p^5$, $5s^25p^44f$ odd- and the $5s5p^6$, $5s5p^54f$, $5s^25p^45d$ even-parity configurations. The orbitals 1s–4f were optimized on the $5s^25p^34f^2$ ground configuration while the 5d orbital was optimized using the MR configurations, keeping all other orbitals fixed. For these two ions, a VV3 model in which the active set included 7s, 7p, 7d, 6f, and 5g orbitals was added to the VV1 and VV2 models described above. From VV3, CV calculations were then carried out by allowing SD excitations from the 4d core orbital to 5s, 5p, 5d, 4f, 5f, and 5g, giving rise to 215 456 and 623 974 CSFs in the odd and even parities of Pr X and to 3767 300 and 622 057 CSFs in the odd and even parities of Pm IX.

In the case of Pr V, Nd V, and Pr X, a comparison of our MCDHF energy level values obtained in CV models revealed a good agreement with the experimental data reported in the literature (Kaufman & Sugar 1967 for Pr V, Meftah et al. 2008; Delghiche et al. 2015 for Nd V, and Bekker et al. 2019 for Pr X), the mean deviation $|\Delta E|/E_{\rm Exp}$ (with $\Delta E = E_{\rm MCDHF} - E_{\rm Exp}$) being found to be equal to 0.018 ± 0.09 (Pr V), 0.006 ± 0.063 (Nd V) and 0.126 ± 0.09 (Pr X).

3.3 AMBIT code

Finally, as third computational procedure, the combination of configuration interaction with many-body perturbation-theory (CI + MBPT) method as implemented in the AMBIT atomic structure code (Kahl & Berengut 2019) was used in order to calculate the level energies and radiative parameters in three representative lanthanide ions, i.e. Pr V, Pr X, and Nd V. Moreover, the emu CI approximation (Geddes et al. 2018) as coded in the AMBIT program was further employed in Pr V so to reduce the size of the problem without losing much accuracy. The details of this theoretical approach were reminded in our previous papers (Carvajal Gallego et al. 2022a, b) and will therefore not be repeated here.

Our AMBIT calculations were focused on the properties of the experimental energy levels found in the literature, i.e. eight levels of Pr V belonging to the configurations 4f, 5d, 6s, 6p, and 7s with symmetries $J^\Pi = 1/2^{\rm odd} - 7/2^{\rm odd}$, $1/2^{\rm even} - 5/2^{\rm even}$ determined by Kaufman & Sugar (1967), 15 levels of Pr X reported by Bekker et al. (2019) and belonging to the even configurations $5s^25p^2$ and $5s^25p4f$ with symmetries $J^\Pi = 0^{\rm even} - 5^{\rm even}$, and 152 levels of Nd V published by Meftah et al. (2008) and by Delghiche et al. (2015) and belonging to the configurations $5s^25p^64f^2$, $5s^25p^64f5d$, $5s^25p^64f6s$, $5s^25p^64f6p$, and $5s^25p^54f^25d$ with symmetries $J^\Pi = 0^{\rm even} - 6^{\rm even}$, $0^{\rm odd} - 7^{\rm odd}$.

Different strategies were followed in our calculations. In Pr V, the core spin-orbitals and the frozen core potential were generated by solving the Dirac–Hartree–Fock (DHF) equations for the Xe-like ground configurations $[Pd]5s^25p^6$ consisting in 54 electrons. The Breit and QED interactions were included. The valence orbitals were determined by diagonalizing a set of *B*-splines using the DHF Hamiltonian with the abovementioned frozen core potential. The emu CI expansions with symmetries $J^\Pi = 1/2^{\rm even} - 5/2^{\rm even}$, $1/2^{\rm odd} - 7/2^{\rm odd}$ were obtained by considering for the large side the single and double electron and hole excitations from leading configurations 4f, 6p, 5d, 6s, and 7s to the active set of orbitals 15spdfgh with all the core orbitals lower than 5s inactive, i.e. 5s to 15s, 5p to 15p, 5d to 15d, 4f to 15f, 5g to 15g, and 6h to 15h. For the small side, the active set of orbitals was reduced to 8spdfgh for the double electron excitations and only single hole excitations were considered. The resulting emu CI matrix dimensions were $N = 9720\,262$ for the large side and $N_{\rm small} = 64\,101$ for the small side. One-, two-, and three-body MBPT diagrams (Berengut, Flambaum & Kozlov 2006) involving the frozen core orbitals and virtual orbitals up to 30spdfgh were considered in the evaluation of the operator matrix elements. The relative differences, $\Delta E = (E_{\rm cal} - E_{\rm exp})/E_{\rm exp}$, with respect to the experimental energy levels published by Kaufman & Sugar (1967) ranged from more than 1–3 per cent with an average of 2.2 per cent and a standard deviation of 0.6 per cent.

Concerning Pr X, the DHF equations were solved in a first step for the ground configuration of the Pd-like Pr XIV system, i.e. $[Kr]4d^{10}$, with 46 electrons in order to obtain the core orbitals. This enabled us to build in a second step the core electron potential and to solve the frozen core DHF equations for the valence orbitals. In both steps, the Breit and QED corrections were included. In the CI step, the 50-electron wavefunction expansions with symmetries $J^\Pi = 0^{\rm even} - 12^{\rm even}$, $0^{\rm odd} - 11^{\rm odd}$ were generated by considering all the single electron excitations from the $5s^25p^2$, $5s^24f^2$, $5s^25p4f$, $5s5p^3$, $5s5p^24f$, $5s5p4f^2$, $5s4f^3$, $5p^4$, $4f^4$, $5p^34f$, $5p4f^3$, and $5p^24f^2$ leading configurations to the 6spd5f active set keeping all the core orbitals lower than 5s inactive. The dimension of the CI matrix was $N = 8\,561$. In the MBPT step, one-, two-, and three-body diagrams were considered involving the frozen core orbitals and virtual orbitals belonging to the set 30spdfgh. Here, the relative differences, ΔE, between our eigenvalues and the available experimental energy levels (Bekker et al. 2019) ranged from −3.4 per cent to 1.3 per cent

Table 5. Transition probabilities (gA) and oscillator strengths (log gf) for experimentally observed lines in Pr V.

λ_{obs} (Å)[a]	Transition[a]		gA (s^{-1})	log gf			
	Lower level	Upper level	HFR + CPOL[b]	HFR + CPOL[b]	MCDHF[b]	AMBIT[b]	Others
843.783	$5s^25p^64f\ ^2F^o_{5/2}$	$5s^25p^65d\ ^2D_{5/2}$	6.78E + 07	− 2.11	− 2.14	− 2.00	− 1.94[d]
							− 1.90[e]
							− 2.05[g]
865.902	$5s^25p^64f\ ^2F^o_{7/2}$	$5s^25p^65d\ ^2D_{5/2}$	1.19E + 09	− 0.83	− 0.86	− 0.70	− 0.64[d]
							− 0.59[e]
							− 0.77[g]
869.170	$5s^25p^64f\ ^2F^o_{5/2}$	$5s^25p^65d\ ^2D_{3/2}$	8.23E + 08	− 0.99	− 1.03	− 0.88	− 0.81[d]
							− 0.76[e]
							− 0.92[g]
869.662	$5s^25p^65d\ ^2D_{3/2}$	$5s^25p^66p\ ^2P^o_{3/2}$	1.33E + 09	− 0.82		− 0.90	− 0.91[d]
							− 0.91[e]
							− 0.81[f]
							− 0.84[g]
896.654	$5s^25p^65d\ ^2D_{5/2}$	$5s^25p^66p\ ^2P^o_{3/2}$	1.10E + 10	0.12		0.07	0.06[d]
							0.06[e]
							0.16[f]
							0.09[g]
922.290	$5s^25p^65d\ ^2D_{3/2}$	$5s^25p^66p\ ^2P^o_{1/2}$	5.74E + 09	− 0.15		− 0.19	− 0.18[d]
							− 0.19[e]
							− 0.08[f]
							− 0.18[g]
1234.070	$5s^25p^66p\ ^2P^o_{1/2}$	$5s^25p^67s\ ^2S_{1/2}$	2.17E + 09	− 0.34		− 0.40	− 0.31[g]
1342.775	$5s^25p^66p\ ^2P^o_{3/2}$	$5s^25p^67s\ ^2S_{1/2}$	3.58E + 09	− 0.07		− 0.01	− 0.04[g]
1958.088	$5s^25p^66s\ ^2S_{1/2}$ ($F = 2$)	$5s^25p^66p\ ^2P^o_{3/2}$	2.28E + 09	0.17		0.18	0.21[c]
							0.17[d]
							0.15[e]
							0.28[f]
							0.21[g]
1958.201	$5s^25p^66s\ ^2S_{1/2}$ ($F = 3$)	$5s^25p^66p\ ^2P^o_{3/2}$	2.28E + 09	0.17		0.18	0.21[c]
							0.17[d]
							0.15[e]
							0.28[f]
							0.21[g]
2246.759	$5s^25p^66s\ ^2S_{1/2}$ ($F = 2$)	$5s^25p^66p\ ^2P^o_{1/2}$	7.86E + 08	− 0.19		− 0.19	− 0.15[c]
							− 0.19[d]
							− 0.21[e]
							− 0.08[f]
							− 0.15[g]
2246.900	$5s^25p^66s\ ^2S_{1/2}$ ($F = 3$)	$5s^25p^66p\ ^2P^o_{1/2}$	7.86E + 08	− 0.19		− 0.19	− 0.15[c]
							− 0.19[d]
							− 0.21[e]
							− 0.08[f]
							− 0.15[g]

[a]Kaufman & Sugar (1967).
[b]This work.
[c]Migdalek & Baylis (1979).
[d]Migdalek & Wyrozunska (1987).
[e]Savukov et al. (2003).
[f]Zilitis (2014).
[g]Karaçoban & Dogan (2015).

with an average of −1.3 per cent and a standard deviation of 1.2 per cent.

In Nd V, the frozen core potential and the corresponding orbitals were determined by solving the DHF equations for the ground configuration of the Xe-like Nd VII, i.e. $[Kr]4d^{10}5s^25p^6$. These were used afterward to solve the frozen-core DHF equations for the 56-electron Nd V atomic system and to obtain the valence orbitals. The CI matrix was built by considering a set of interacting configurations with symmetries $J^\Pi = 0^{even} - 6^{even}, 0^{odd} - 5^{odd}$ generated by single and double electron and hole excitations to the 6spdfg active set of orbitals from the leading configurations $4f^2$ and 4f5d keeping inactive the orbitals of the Pd-like Nd XV frozen core, i.e. from 1s up to 4d. The dimension of the CI matrix was $N = 1708\,459$. Finally, the MBPT corrections were added to the projected effective multielectron Hamiltonian matrix by evaluating the one-, two-, and three-body diagrams involving the Pd-like frozen core orbitals and virtual orbitals up to 30spdfgh. The relative differences with the experimental level energies of Meftah et al. (2008) and Delghiche

Table 6. Transition probabilities (gA) and oscillator strengths (log gf) for experimentally observed lines in Nd V.

λ_{obs} (Å)[a]	Transition		gA (s^{-1})		log gf
	Lower level	Upper level	Previous[a]	HFR + CPOL[b]	HFR + CPOL[b]
370.698	$5s^25p^64f^2$ 5743.4 ($J = 6$)	$5s^25p^54f^25d$ 275504.9 ($J = 5$)^o	4.19E + 11	1.09E + 11	0.30
371.855	$5s^25p^64f^2$ 2834.3 ($J = 5$)	$5s^25p^54f^25d$ 271756.6 ($J = 4$)^o	1.80E + 11	4.02E + 09	− 1.11
372.550	$5s^25p^64f^2$ 7784.8 ($J = 3$)	$5s^25p^54f^25d$ 276205.0 ($J = 2$)^o	3.78E + 11	9.70E + 10	1.05
372.828	$5s^25p^64f^2$ 8311.4 ($J = 4$)	$5s^25p^54f^25d$ 276531.3 ($J = 4$)^o	6.42E + 11	4.77E + 07	− 2.98
373.070	$5s^25p^64f^2$ 7784.8 ($J = 3$)	$5s^25p^54f^25d$ 275831.0 ($J = 3$)^o	4.91E + 11	6.10E + 10	1.06
373.564	$5s^25p^64f^2$ 5893.8 ($J = 2$)	$5s^25p^54f^25d$ 273585.8 ($J = 3$)^o	4.22E + 11	3.18E + 08	− 2.22
373.819	$5s^25p^64f^2$ 5743.4 ($J = 6$)	$5s^25p^54f^25d$ 273256.0 ($J = 5$)^o	1.03E + 12	1.23E + 12	1.36
374.261	$5s^25p^64f^2$ 8311.4 ($J = 4$)	$5s^25p^54f^25d$ 275504.9 ($J = 5$)^o	8.80E + 11	2.35E + 11	0.64
374.390	$5s^25p^64f^2$ 26088.1 ($J = 6$)	$5s^25p^54f^25d$ 293189.0 ($J = 7$)^o	1.86E + 12	3.64E + 08	− 2.19
374.658	$5s^25p^64f^2$ 7784.8 ($J = 3$)	$5s^25p^54f^25d$ 274695.0 ($J = 4$)^o	9.85E + 11	8.36E + 11	1.19
374.930	$5s^25p^64f^2$ 12269.7 ($J = 4$)	$5s^25p^54f^25d$ 278986.5 ($J = 4$)^o	1.06E + 12	2.00E + 09	− 1.41
375.151	$5s^25p^64f^2$ 7784.8 ($J = 3$)	$5s^25p^54f^25d$ 274344.0 ($J = 3$)^o	1.64E + 11	4.68E + 08	− 1.53
375.451	$5s^25p^64f^2$ 0.0 ($J = 4$)	$5s^25p^54f^25d$ 266346.0 ($J = 5$)^o	1.32E + 12	1.47E + 12	1.44
375.641	$5s^25p^64f^2$ 2834.3 ($J = 5$)	$5s^25p^54f^25d$ 269046.0 ($J = 6$)^o	1.57E + 12	1.73E + 12	1.51
375.641	$5s^25p^64f^2$ 5743.4 ($J = 6$)	$5s^25p^54f^25d$ 271955.0 ($J = 7$)^o	1.78E + 12	2.00E + 12	1.57
376.458	$5s^25p^64f^2$ 2834.3 ($J = 5$)	$5s^25p^54f^25d$ 268468.0 ($J = 5$)^o	7.91E + 11	2.22E + 06	− 4.40
377.058	$5s^25p^64f^2$ 5743.4 ($J = 6$)	$5s^25p^54f^25d$ 270954.6 ($J = 6$)^o	1.59E + 12	1.71E + 12	1.51
377.432	$5s^25p^64f^2$ 8311.4 ($J = 4$)	$5s^25p^54f^25d$ 273256.0 ($J = 5$)^o	3.94E + 11	1.59E + 11	0.48
408.012	$5s^25p^64f^2$ 8311.4 ($J = 4$)	$5s^25p^54f^25d$ 253402.8 ($J = 5$)^o	6.87E + 09	6.27E + 06	− 3.85
412.657	$5s^25p^64f^2$ 2834.3 ($J = 5$)	$5s^25p^54f^25d$ 245165.8 ($J = 6$)^o	2.48E + 09	7.70E + 08	− 1.73
412.734	$5s^25p^64f^2$ 5743.4 ($J = 6$)	$5s^25p^54f^25d$ 248026.8 ($J = 7$)^o	1.67E + 09	4.86E + 09	− 0.82
413.770	$5s^25p^64f^2$ 0.0 ($J = 4$)	$5s^25p^54f^25d$ 241677.8 ($J = 3$)^o	1.16E + 09	4.17E + 07	− 3.00
417.562	$5s^25p^64f^2$ 0.0 ($J = 4$)	$5s^25p^54f^25d$ 239482.1 ($J = 3$)^o	3.24E + 09	1.92E + 08	− 2.33
420.851	$5s^25p^64f^2$ 5743.4 ($J = 6$)	$5s^25p^54f^25d$ 243355.7 ($J = 7$)^o	1.43E + 10	1.36E + 10	− 0.45
421.607	$5s^25p^64f^2$ 0.0 ($J = 4$)	$5s^25p^54f^25d$ 237184.8 ($J = 3$)^o	1.60E + 09	3.67E + 09	− 1.10
424.125	$5s^25p^64f^2$ 5893.8 ($J = 2$)	$5s^25p^54f^25d$ 241677.8 ($J = 3$)^o	2.98E + 09	8.89E + 11	1.22
427.543	$5s^25p^64f^2$ 7784.8 ($J = 3$)	$5s^25p^54f^25d$ 241677.8 ($J = 3$)^o	2.11E + 09	2.84E + 09	− 1.27
427.680	$5s^25p^64f^2$ 0.0 ($J = 4$)	$5s^25p^54f^25d$ 233817.4 ($J = 3$)^o	3.28E + 09	6.65E + 09	− 0.71
428.117	$5s^25p^64f^2$ 0.0 ($J = 4$)	$5s^25p^54f^25d$ 233581.0 ($J = 5$)^o	5.62E + 09	1.54E + 09	− 1.37
429.107	$5s^25p^64f^2$ 5743.4 ($J = 6$)	$5s^25p^54f^25d$ 238787.0 ($J = 7$)^o	1.21E + 09	2.32E + 07	− 3.20
430.296	$5s^25p^64f^2$ 5893.8 ($J = 2$)	$5s^25p^54f^25d$ 238294.8 ($J = 3$)^o	3.45E + 08	3.88E + 08	− 2.01
430.601	$5s^25p^64f^2$ 5893.8 ($J = 2$)	$5s^25p^54f^25d$ 238127.6 ($J = 2$)^o	1.91E + 09	5.86E + 07	− 2.81
431.594	$5s^25p^64f^2$ 7784.8 ($J = 3$)	$5s^25p^54f^25d$ 239482.1 ($J = 3$)^o	1.25E + 09	2.12E + 07	− 3.23
432.356	$5s^25p^64f^2$ 0.0 ($J = 4$)	$5s^25p^54f^25d$ 231296.1 ($J = 4$)^o	3.88E + 09	5.82E + 09	− 0.75
432.356	$5s^25p^64f^2$ 5893.8 ($J = 2$)	$5s^25p^54f^25d$ 237184.8 ($J = 3$)^o	3.18E + 09	8.14E + 06	− 3.59
432.389	$5s^25p^64f^2$ 2834.3 ($J = 5$)	$5s^25p^54f^25d$ 234105.4 ($J = 5$)^o	1.65E + 09	2.51E + 09	− 1.13
432.448	$5s^25p^64f^2$ 0.0 ($J = 4$)	$5s^25p^54f^25d$ 231240.8 ($J = 4$)^o	8.12E + 08	3.02E + 08	− 2.13
432.577	$5s^25p^64f^2$ 8311.4 ($J = 4$)	$5s^25p^54f^25d$ 239482.1 ($J = 3$)^o	9.20E + 08	8.96E + 08	− 1.62
432.810	$5s^25p^64f^2$ 0.0 ($J = 4$)	$5s^25p^54f^25d$ 231046.4 ($J = 3$)^o	1.52E + 09	1.10E + 09	− 1.52
432.960	$5s^25p^64f^2$ 0.0 ($J = 4$)	$5s^25p^54f^25d$ 230967.9 ($J = 5$)^o	8.52E + 09	3.21E + 06	− 4.05
433.130	$5s^25p^64f^2$ 7784.8 ($J = 3$)	$5s^25p^54f^25d$ 238661.2 ($J = 4$)^o	3.32E + 09	1.54E + 09	− 1.32
433.130	$5s^25p^64f^2$ 8311.4 ($J = 4$)	$5s^25p^54f^25d$ 239188.9 ($J = 3$)^o	3.16E + 09	1.97E + 08	− 2.29
433.366	$5s^25p^64f^2$ 2834.3 ($J = 5$)	$5s^25p^54f^25d$ 233581.0 ($J = 5$)^o	3.25E + 09	1.65E + 08	− 2.33
433.820	$5s^25p^64f^2$ 7784.8 ($J = 3$)	$5s^25p^54f^25d$ 238294.8 ($J = 3$)^o	4.08E + 08	5.84E + 08	− 1.82
434.131	$5s^25p^64f^2$ 7784.8 ($J = 3$)	$5s^25p^54f^25d$ 238127.6 ($J = 2$)^o	2.45E + 09	1.83E + 09	− 1.31
434.350	$5s^25p^64f^2$ 5743.4 ($J = 6$)	$5s^25p^54f^25d$ 235965.1 ($J = 5$)^o	6.99E + 08	4.40E + 08	− 1.87
434.808	$5s^25p^64f^2$ 8311.4 ($J = 4$)	$5s^25p^54f^25d$ 238294.8 ($J = 3$)^o	7.51E + 08	5.19E + 08	− 1.88
436.840	$5s^25p^64f^2$ 26088.1 ($J = 6$)	$5s^25p^54f^25d$ 255005.0 ($J = 7$)^o	3.63E + 10	9.07E + 08	− 1.49
437.166	$5s^25p^64f^2$ 0.0 ($J = 4$)	$5s^25p^54f^25d$ 228737.2 ($J = 4$)^o	5.69E + 08	1.00E + 09	− 1.69
437.401	$5s^25p^64f^2$ 0.0 ($J = 4$)	$5s^25p^54f^25d$ 228623.7 ($J = 5$)^o	1.53E + 09	1.25E + 09	− 1.46
437.711	$5s^25p^64f^2$ 2834.3 ($J = 5$)	$5s^25p^54f^25d$ 231296.1 ($J = 4$)^o	1.15E + 08	1.86E + 08	− 2.23
437.812	$5s^25p^64f^2$ 2834.3 ($J = 5$)	$5s^25p^54f^25d$ 231240.8 ($J = 4$)^o	8.62E + 09	3.72E + 08	− 1.97
437.897	$5s^25p^64f^2$ 5743.4 ($J = 6$)	$5s^25p^54f^25d$ 234105.4 ($J = 5$)^o	4.79E + 09	2.86E + 09	− 1.06
438.228	$5s^25p^64f^2$ 0.0 ($J = 4$)	$5s^25p^54f^25d$ 228189.8 ($J = 3$)^o	5.54E + 09	1.10E + 09	− 1.52
438.228	$5s^25p^64f^2$ 5743.4 ($J = 6$)	$5s^25p^54f^25d$ 233935.4 ($J = 7$)^o	1.01E + 10	8.47E + 08	− 1.60
438.430	$5s^25p^64f^2$ 5893.8 ($J = 2$)	$5s^25p^54f^25d$ 233979.7 ($J = 2$)^o	3.75E + 08	4.34E + 08	− 1.92
438.742	$5s^25p^64f^2$ 5893.8 ($J = 2$)	$5s^25p^54f^25d$ 233817.4 ($J = 3$)^o	5.89E + 09	8.00E + 08	− 1.64
438.913	$5s^25p^64f^2$ 5743.4 ($J = 6$)	$5s^25p^54f^25d$ 233581.0 ($J = 5$)^o	2.45E + 09	2.45E + 09	− 1.15
439.265	$5s^25p^64f^2$ 8311.4 ($J = 4$)	$5s^25p^54f^25d$ 235965.1 ($J = 5$)^o	2.68E + 09	4.66E + 08	− 1.83
439.918	$5s^25p^64f^2$ 26088.1 ($J = 6$)	$5s^25p^54f^25d$ 253402.8 ($J = 5$)^o	2.05E + 10	9.61E + 09	− 0.61
440.129	$5s^25p^64f^2$ 12269.7 ($J = 4$)	$5s^25p^54f^25d$ 239482.1 ($J = 3$)^o	3.19E + 09	2.96E + 09	− 1.08
440.424	$5s^25p^64f^2$ 0.0 ($J = 4$)	$5s^25p^54f^25d$ 227051.0 ($J = 3$)^o	3.84E + 09	3.96E + 08	− 1.93
440.685	$5s^25p^64f^2$ 12269.7 ($J = 4$)	$5s^25p^54f^25d$ 239188.9 ($J = 3$)^o	1.79E + 09	2.96E + 09	− 1.08
441.124	$5s^25p^64f^2$ 2834.3 ($J = 5$)	$5s^25p^54f^25d$ 229533.7 ($J = 4$)^o	2.28E + 09	1.06E + 09	− 1.42

Table 6 – *continued*

λ_{obs} (Å)[a]	Transition		gA (s^{-1})		log gf
	Lower level	Upper level	Previous[a]	HFR + CPOL[b]	HFR + CPOL[b]
441.268	$5s^25p^64f^2$ 0.0 ($J = 4$)	$5s^25p^54f^25d$ 226618.2 ($J = 5$)^o	1.22E + 10	2.16E + 09	− 1.21
441.679	$5s^25p^64f^2$ 0.0 ($J = 4$)	$5s^25p^54f^25d$ 226411.4 ($J = 5$)^o	2.24E + 07	3.40E + 08	− 2.02
441.714	$5s^25p^64f^2$ 12269.7 ($J = 4$)	$5s^25p^54f^25d$ 238661.2 ($J = 4$)^o	1.16E + 10	6.44E + 08	− 1.72
441.876	$5s^25p^64f^2$ 26088.1 ($J = 6$)	$5s^25p^54f^25d$ 252396.0 ($J = 7$)^o	2.64E + 10	4.15E + 10	0.06
442.097	$5s^25p^64f^2$ 7784.8 ($J = 3$)	$5s^25p^54f^25d$ 233979.7 ($J = 2$)^o	1.08E + 09	1.44E + 08	− 2.39
442.216	$5s^25p^64f^2$ 0.0 ($J = 4$)	$5s^25p^54f^25d$ 226134.9 ($J = 3$)^o	2.88E + 08	3.83E + 08	− 1.99
442.424	$5s^25p^64f^2$ 7784.8 ($J = 3$)	$5s^25p^54f^25d$ 233817.4 ($J = 3$)^o	7.09E + 09	1.35E + 09	− 1.41
442.424	$5s^25p^64f^2$ 12269.7 ($J = 4$)	$5s^25p^54f^25d$ 238294.8 ($J = 3$)^o	7.25E + 09	7.96E + 07	− 2.68
442.678	$5s^25p^64f^2$ 2834.3 ($J = 5$)	$5s^25p^54f^25d$ 228737.2 ($J = 4$)^o	3.99E + 09	3.25E + 09	− 1.04
442.878	$5s^25p^64f^2$ 2834.3 ($J = 5$)	$5s^25p^54f^25d$ 228623.7 ($J = 5$)^o	1.53E + 09	3.31E + 08	− 2.03
442.878	$5s^25p^64f^2$ 8311.4 ($J = 4$)	$5s^25p^54f^25d$ 234105.4 ($J = 5$)^o	1.10E + 09	1.54E + 09	− 1.32
443.066	$5s^25p^64f^2$ 5893.8 ($J = 2$)	$5s^25p^54f^25d$ 231592.0 ($J = 3$)^o	1.29E + 09	4.09E + 08	− 1.95
443.333	$5s^25p^64f^2$ 2834.3 ($J = 5$)	$5s^25p^54f^25d$ 228398.8 ($J = 6$)^o	2.96E + 09	8.57E + 09	− 0.58
444.621	$5s^25p^64f^2$ 12269.7 ($J = 4$)	$5s^25p^54f^25d$ 237184.8 ($J = 3$)^o	1.93E + 09	1.15E + 09	− 1.52
445.375	$5s^25p^64f^2$ 0.0 ($J = 4$)	$5s^25p^54f^25d$ 224529.3 ($J = 4$)^o	3.22E + 09	5.02E + 08	− 1.84
446.855	$5s^25p^64f^2$ 2834.3 ($J = 5$)	$5s^25p^54f^25d$ 226618.2 ($J = 5$)^o	3.70E + 09	2.59E + 09	− 1.11
447.040	$5s^25p^64f^2$ 12269.7 ($J = 4$)	$5s^25p^54f^25d$ 235965.1 ($J = 5$)^o	3.04E + 09	2.11E + 08	− 2.16
447.401	$5s^25p^64f^2$ 7784.8 ($J = 3$)	$5s^25p^54f^25d$ 231296.1 ($J = 4$)^o	3.54E + 08	3.93E + 08	− 1.89
447.514	$5s^25p^64f^2$ 7784.8 ($J = 3$)	$5s^25p^54f^25d$ 231240.8 ($J = 4$)^o	2.51E + 09	2.25E + 09	− 1.17
447.875	$5s^25p^64f^2$ 8311.4 ($J = 4$)	$5s^25p^54f^25d$ 231592.0 ($J = 3$)^o	2.21E + 09	1.97E + 08	− 2.29
447.920	$5s^25p^64f^2$ 0.0 ($J = 4$)	$5s^25p^54f^25d$ 223252.7 ($J = 3$)^o	4.92E + 08	6.49E + 08	− 1.70
448.450	$5s^25p^64f^2$ 8311.4 ($J = 4$)	$5s^25p^54f^25d$ 231296.1 ($J = 4$)^o	2.62E + 09	6.03E + 09	− 0.77
448.572	$5s^25p^64f^2$ 8311.4 ($J = 4$)	$5s^25p^54f^25d$ 231240.8 ($J = 4$)^o	2.68E + 09	3.00E + 08	− 2.05
448.671	$5s^25p^64f^2$ 5743.4 ($J = 6$)	$5s^25p^54f^25d$ 228623.7 ($J = 5$)^o	1.93E + 10	8.51E + 09	− 0.61
448.967	$5s^25p^64f^2$ 8311.4 ($J = 4$)	$5s^25p^54f^25d$ 231046.4 ($J = 3$)^o	1.81E + 09	1.34E + 10	− 0.39
449.123	$5s^25p^64f^2$ 5743.4 ($J = 6$)	$5s^25p^54f^25d$ 228398.8 ($J = 6$)^o	5.63E + 09	8.33E + 08	− 1.61
449.123	$5s^25p^64f^2$ 8311.4 ($J = 4$)	$5s^25p^54f^25d$ 230967.9 ($J = 5$)^o	2.48E + 09	3.83E + 08	− 1.90
449.506	$5s^25p^64f^2$ 0.0 ($J = 4$)	$5s^25p^54f^25d$ 222466.9 ($J = 4$)^o	1.59E + 09	2.57E + 08	− 2.11
449.845	$5s^25p^64f^2$ 5893.8 ($J = 2$)	$5s^25p^54f^25d$ 228189.8 ($J = 3$)^o	4.01E + 09	1.54E + 09	− 1.35
450.322	$5s^25p^64f^2$ 0.0 ($J = 4$)	$5s^25p^54f^25d$ 222061.2 ($J = 5$)^o	1.08E + 09	7.72E + 07	− 2.72
450.580	$5s^25p^64f^2$ 26088.1 ($J = 6$)	$5s^25p^54f^25d$ 248026.8 ($J = 7$)^o	1.55E + 10	4.86E + 09	− 0.82
450.781	$5s^25p^64f^2$ 12269.7 ($J = 4$)	$5s^25p^54f^25d$ 234105.4 ($J = 5$)^o	5.67E + 07	5.01E + 08	− 1.79
450.968	$5s^25p^64f^2$ 7784.8 ($J = 3$)	$5s^25p^54f^25d$ 229533.7 ($J = 4$)^o	2.70E + 09	1.07E + 08	− 2.53
451.077	$5s^25p^64f^2$ 2834.3 ($J = 5$)	$5s^25p^54f^25d$ 224529.3 ($J = 4$)^o	2.41E + 09	1.06E + 09	− 1.50
451.217	$5s^25p^64f^2$ 2834.3 ($J = 5$)	$5s^25p^54f^25d$ 224461.6 ($J = 6$)^o	2.11E + 08	5.47E + 08	− 1.81
451.371	$5s^25p^64f^2$ 12269.7 ($J = 4$)	$5s^25p^54f^25d$ 233817.4 ($J = 3$)^o	1.12E + 09	8.65E + 07	− 2.59
451.640	$5s^25p^64f^2$ 0.0 ($J = 4$)	$5s^25p^54f^25d$ 221416.7 ($J = 3$)^o	2.62E + 08	4.91E + 08	− 1.85
451.858	$5s^25p^64f^2$ 12269.7 ($J = 4$)	$5s^25p^54f^25d$ 233581.0 ($J = 5$)^o	2.20E + 10	5.79E + 09	− 0.79
452.015	$5s^25p^64f^2$ 8311.4 ($J = 4$)	$5s^25p^54f^25d$ 229533.7 ($J = 4$)^o	8.67E + 09	2.65E + 08	− 2.13
452.228	$5s^25p^64f^2$ 20551.4 ($J = 2$)	$5s^25p^54f^25d$ 241677.8 ($J = 3$)^o	1.18E + 09	1.83E + 08	− 2.24
452.406	$5s^25p^64f^2$ 0.0 ($J = 4$)	$5s^25p^54f^25d$ 221040.4 ($J = 3$)^o	1.65E + 10	3.10E + 07	− 3.00
452.524	$5s^25p^64f^2$ 8311.4 ($J = 4$)	$5s^25p^54f^25d$ 229292.9 ($J = 5$)^o	1.32E + 10	7.46E + 09	− 0.65
452.600	$5s^25p^64f^2$ 7784.8 ($J = 3$)	$5s^25p^54f^25d$ 228737.2 ($J = 4$)^o	4.21E + 09	4.08E + 08	− 1.92
452.744	$5s^25p^64f^2$ 5743.4 ($J = 6$)	$5s^25p^54f^25d$ 226618.2 ($J = 5$)^o	5.27E + 09	1.13E + 09	− 1.47
452.881	$5s^25p^64f^2$ 2834.3 ($J = 5$)	$5s^25p^54f^25d$ 223644.5 ($J = 6$)^o	4.51E + 09	5.47E + 08	− 1.81
452.991	$5s^25p^64f^2$ 0.0 ($J = 4$)	$5s^25p^54f^25d$ 220754.5 ($J = 4$)^o	4.74E + 08	1.32E + 08	− 2.45
453.176	$5s^25p^64f^2$ 5743.4 ($J = 6$)	$5s^25p^54f^25d$ 226411.4 ($J = 5$)^o	2.40E + 09	5.34E + 08	− 1.80
453.176	$5s^25p^64f^2$ 5743.4 ($J = 6$)	$5s^25p^54f^25d$ 226271.3 ($J = 7$)^o	4.60E + 10	2.05E + 10	− 0.21
453.562	$5s^25p^64f^2$ 0.0 ($J = 4$)	$5s^25p^54f^25d$ 220472.9 ($J = 5$)^o	5.78E + 07	1.73E + 09	− 1.28
453.659	$5s^25p^64f^2$ 8311.4 ($J = 4$)	$5s^25p^54f^25d$ 228737.2 ($J = 4$)^o	6.99E + 08	6.58E + 08	− 1.73
453.914	$5s^25p^64f^2$ 8311.4 ($J = 4$)	$5s^25p^54f^25d$ 228623.7 ($J = 5$)^o	6.13E + 08	2.77E + 09	− 1.08
454.053	$5s^25p^64f^2$ 2834.3 ($J = 5$)	$5s^25p^54f^25d$ 223069.0 ($J = 4$)^o	6.70E + 09	1.45E + 09	− 1.37
454.053	$5s^25p^64f^2$ 5893.8 ($J = 2$)	$5s^25p^54f^25d$ 226134.9 ($J = 3$)^o	2.27E + 09	8.79E + 08	− 1.60
454.702	$5s^25p^64f^2$ 5743.4 ($J = 6$)	$5s^25p^54f^25d$ 225668.8 ($J = 5$)^o	4.76E + 09	6.18E + 07	− 2.69
454.791	$5s^25p^64f^2$ 2834.3 ($J = 5$)	$5s^25p^54f^25d$ 222716.4 ($J = 5$)^o	4.27E + 09	6.83E + 09	− 0.68
455.194	$5s^25p^64f^2$ 0.0 ($J = 4$)	$5s^25p^54f^25d$ 219685.7 ($J = 4$)^o	2.91E + 09	1.42E + 10	− 0.37
455.194	$5s^25p^64f^2$ 5893.8 ($J = 2$)	$5s^25p^54f^25d$ 225576.7 ($J = 3$)^o	6.10E + 09	2.74E + 09	− 1.08
455.318	$5s^25p^64f^2$ 2834.3 ($J = 5$)	$5s^25p^54f^25d$ 222466.9 ($J = 4$)^o	8.27E + 08	7.02E + 08	− 1.71
455.954	$5s^25p^64f^2$ 12269.7 ($J = 4$)	$5s^25p^54f^25d$ 231592.0 ($J = 3$)^o	1.13E + 09	1.02E + 09	− 1.53
456.059	$5s^25p^64f^2$ 7784.8 ($J = 3$)	$5s^25p^54f^25d$ 227051.0 ($J = 3$)^o	2.77E + 09	1.47E + 09	− 1.53
456.398	$5s^25p^64f^2$ 0.0 ($J = 4$)	$5s^25p^54f^25d$ 219103.5 ($J = 5$)^o	1.40E + 10	4.29E + 09	− 0.89
456.460	$5s^25p^64f^2$ 26088.1 ($J = 6$)	$5s^25p^54f^25d$ 245165.8 ($J = 6$)^o	9.23E + 09	5.04E + 09	− 0.81
456.575	$5s^25p^64f^2$ 12269.7 ($J = 4$)	$5s^25p^54f^25d$ 231296.1 ($J = 4$)^o	1.08E + 09	6.18E + 08	− 1.72
456.688	$5s^25p^64f^2$ 12269.7 ($J = 4$)	$5s^25p^54f^25d$ 231240.8 ($J = 4$)^o	7.24E + 08	5.64E + 08	− 1.75

Table 6 – *continued*

λ_{obs} (Å)[a]	Transition		gA (s^{-1})		log gf
	Lower level	Upper level	Previous[a]	HFR + CPOL[b]	HFR + CPOL[b]
456.765	$5s^25p^64f^2$ 20551.4 ($J = 2$)	$5s^25p^54f^25d$ 239482.1 ($J = 3$)^o	2.57E + 08	1.03E + 09	− 1.48
457.171	$5s^25p^64f^2$ 8311.4 ($J = 4$)	$5s^25p^54f^25d$ 227051.0 ($J = 3$)^o	2.80E + 09	1.76E + 08	− 2.25
457.212	$5s^25p^64f^2$ 5743.4 ($J = 6$)	$5s^25p^54f^25d$ 224461.6 ($J = 6$)^o	2.67E + 10	5.20E + 08	− 1.82
457.380	$5s^25p^64f^2$ 0.0 ($J = 4$)	$5s^25p^54f^25d$ 218638.7 ($J = 5$)^o	1.97E + 08	1.73E + 09	− 1.28
457.380	$5s^25p^64f^2$ 2834.3 ($J = 5$)	$5s^25p^54f^25d$ 221468.6 ($J = 6$)^o	1.27E + 09	1.28E + 09	− 1.41
457.380	$5s^25p^64f^2$ 20551.4 ($J = 2$)	$5s^25p^54f^25d$ 239188.9 ($J = 3$)^o	8.40E + 08	1.39E + 08	− 2.45
457.939	$5s^25p^64f^2$ 0.0 ($J = 4$)	$5s^25p^54f^25d$ 218371.0 ($J = 4$)^o	4.76E + 09	3.34E + 08	− 2.02
458.099	$5s^25p^64f^2$ 5893.8 ($J = 2$)	$5s^25p^54f^25d$ 224181.2 ($J = 2$)^o	7.18E + 08	1.76E + 08	− 2.27
458.498	$5s^25p^64f^2$ 8311.4 ($J = 4$)	$5s^25p^54f^25d$ 226411.4 ($J = 5$)^o	3.39E + 09	2.35E + 09	− 1.14
458.674	$5s^25p^64f^2$ 5893.8 ($J = 2$)	$5s^25p^54f^25d$ 223914.6 ($J = 3$)^o	6.30E + 09	1.21E + 08	− 2.49
458.885	$5s^25p^64f^2$ 0.0 ($J = 4$)	$5s^25p^54f^25d$ 217916.4 ($J = 4$)^o	1.47E + 10	1.10E + 09	− 1.47
458.885	$5s^25p^64f^2$ 2834.3 ($J = 5$)	$5s^25p^54f^25d$ 220754.5 ($J = 4$)^o	1.83E + 09	7.02E + 08	− 1.71
458.921	$5s^25p^64f^2$ 5743.4 ($J = 6$)	$5s^25p^54f^25d$ 223644.5 ($J = 6$)^o	1.06E + 10	5.20E + 08	− 1.82
459.087	$5s^25p^64f^2$ 8311.4 ($J = 4$)	$5s^25p^54f^25d$ 226134.9 ($J = 3$)^o	5.39E + 09	5.87E + 08	− 1.77
459.157	$5s^25p^64f^2$ 7784.8 ($J = 3$)	$5s^25p^54f^25d$ 225576.7 ($J = 3$)^o	7.95E + 08	2.04E + 09	− 1.22
459.461	$5s^25p^64f^2$ 2834.3 ($J = 5$)	$5s^25p^54f^25d$ 220472.9 ($J = 5$)^o	2.06E + 10	3.17E + 09	− 1.00
459.606	$5s^25p^64f^2$ 20551.4 ($J = 2$)	$5s^25p^54f^25d$ 238127.6 ($J = 2$)^o	1.92E + 09	3.06E + 08	− 2.03
460.074	$5s^25p^64f^2$ 5893.8 ($J = 2$)	$5s^25p^54f^25d$ 223252.7 ($J = 3$)^o	3.29E + 09	2.27E + 09	− 1.16
460.074	$5s^25p^64f^2$ 8311.4 ($J = 4$)	$5s^25p^54f^25d$ 225668.8 ($J = 5$)^o	1.67E + 09	1.50E + 08	− 2.29
460.106	$5s^25p^64f^2$ 0.0 ($J = 4$)	$5s^25p^54f^25d$ 217341.6 ($J = 4$)^o	5.52E + 09	4.41E + 08	− 1.92
460.267	$5s^25p^64f^2$ 8311.4 ($J = 4$)	$5s^25p^54f^25d$ 225576.7 ($J = 3$)^o	7.72E + 08	7.56E + 08	− 1.65
460.267	$5s^25p^64f^2$ 26088.1 ($J = 6$)	$5s^25p^54f^25d$ 243355.7 ($J = 7$)^o	7.42E + 09	5.42E + 08	− 1.80
460.783	$5s^25p^64f^2$ 12269.7 ($J = 4$)	$5s^25p^54f^25d$ 229292.9 ($J = 5$)^o	4.55E + 09	2.41E + 09	− 1.13
460.898	$5s^25p^64f^2$ 5743.4 ($J = 6$)	$5s^25p^54f^25d$ 222716.4 ($J = 5$)^o	2.52E + 09	1.35E + 08	− 2.42
461.089	$5s^25p^64f^2$ 5893.8 ($J = 2$)	$5s^25p^54f^25d$ 222773.5 ($J = 2$)^o	7.86E + 08	1.76E + 08	− 2.27
461.152	$5s^25p^64f^2$ 2834.3 ($J = 5$)	$5s^25p^54f^25d$ 219685.7 ($J = 4$)^o	1.62E + 09	6.86E + 08	− 1.67
461.366	$5s^25p^64f^2$ 7784.8 ($J = 3$)	$5s^25p^54f^25d$ 224529.3 ($J = 4$)^o	5.60E + 09	1.53E + 09	− 1.32
461.605	$5s^25p^64f^2$ 20551.4 ($J = 2$)	$5s^25p^54f^25d$ 237184.8 ($J = 3$)^o	8.04E + 09	3.72E + 09	− 0.98
461.893	$5s^25p^64f^2$ 0.0 ($J = 4$)	$5s^25p^54f^25d$ 216499.5 ($J = 5$)^o	7.64E + 09	2.19E + 09	− 1.16
462.118	$5s^25p^64f^2$ 7784.8 ($J = 3$)	$5s^25p^54f^25d$ 224181.2 ($J = 2$)^o	1.25E + 09	1.92E + 08	− 2.22
462.199	$5s^25p^64f^2$ 12269.7 ($J = 4$)	$5s^25p^54f^25d$ 228623.7 ($J = 5$)^o	1.53E + 09	3.96E + 09	− 0.94
462.276	$5s^25p^64f^2$ 5743.4 ($J = 6$)	$5s^25p^54f^25d$ 222061.2 ($J = 5$)^o	5.74E + 08	1.14E + 08	− 2.52
462.387	$5s^25p^64f^2$ 2834.3 ($J = 5$)	$5s^25p^54f^25d$ 219103.5 ($J = 5$)^o	3.78E + 09	1.42E + 09	− 1.35
463.138	$5s^25p^64f^2$ 12269.7 ($J = 4$)	$5s^25p^54f^25d$ 228189.8 ($J = 3$)^o	1.95E + 09	5.35E + 08	− 1.78
463.276	$5s^25p^64f^2$ 26088.1 ($J = 6$)	$5s^25p^54f^25d$ 241942.1 ($J = 6$)^o	1.15E + 10	2.31E + 09	− 1.13
463.315	$5s^25p^64f^2$ 0.0 ($J = 4$)	$5s^25p^54f^25d$ 215828.5 ($J = 5$)^o	2.86E + 09	1.25E + 09	− 1.41
463.375	$5s^25p^64f^2$ 2834.3 ($J = 5$)	$5s^25p^54f^25d$ 218638.7 ($J = 5$)^o	4.48E + 09	3.17E + 09	− 1.00
463.554	$5s^25p^64f^2$ 5743.4 ($J = 6$)	$5s^25p^54f^25d$ 221468.6 ($J = 6$)^o	4.14E + 09	2.65E + 09	− 1.08
463.814	$5s^25p^64f^2$ 8311.4 ($J = 4$)	$5s^25p^54f^25d$ 223914.6 ($J = 3$)^o	3.19E + 09	1.13E + 08	− 2.53
463.987	$5s^25p^64f^2$ 2834.3 ($J = 5$)	$5s^25p^54f^25d$ 218353.2 ($J = 6$)^o	2.81E + 09	1.93E + 09	− 1.21
463.987	$5s^25p^64f^2$ 5893.8 ($J = 2$)	$5s^25p^54f^25d$ 221416.7 ($J = 3$)^o	3.18E + 08	9.31E + 08	− 1.55
464.102	$5s^25p^64f^2$ 7784.8 ($J = 3$)	$5s^25p^54f^25d$ 223252.7 ($J = 3$)^o	2.38E + 08	1.93E + 08	− 2.22
464.128	$5s^25p^64f^2$ 0.0 ($J = 4$)	$5s^25p^54f^25d$ 215456.7 ($J = 5$)^o	3.83E + 09	2.19E + 09	− 1.16
464.500	$5s^25p^64f^2$ 7784.8 ($J = 3$)	$5s^25p^54f^25d$ 223069.0 ($J = 4$)^o	7.56E + 09	1.63E + 07	− 3.30
464.810	$5s^25p^64f^2$ 5893.8 ($J = 2$)	$5s^25p^54f^25d$ 221040.4 ($J = 3$)^o	6.49E + 09	8.86E + 08	− 1.51
464.944	$5s^25p^64f^2$ 2834.3 ($J = 5$)	$5s^25p^54f^25d$ 217916.4 ($J = 4$)^o	7.01E + 08	2.14E + 09	− 1.20
465.504	$5s^25p^64f^2$ 7784.8 ($J = 3$)	$5s^25p^54f^25d$ 222602.3 ($J = 3$)^o	1.62E + 09	1.47E + 09	− 1.53
465.596	$5s^25p^64f^2$ 12269.7 ($J = 4$)	$5s^25p^54f^25d$ 227051.0 ($J = 3$)^o	1.47E + 09	2.61E + 09	− 1.27
465.647	$5s^25p^64f^2$ 8311.4 ($J = 4$)	$5s^25p^54f^25d$ 223069.0 ($J = 4$)^o	1.84E + 08	3.54E + 06	− 3.96
465.714	$5s^25p^64f^2$ 5743.4 ($J = 6$)	$5s^25p^54f^25d$ 220472.9 ($J = 5$)^o	1.89E + 09	4.26E + 08	− 1.86
465.802	$5s^25p^64f^2$ 7784.8 ($J = 3$)	$5s^25p^54f^25d$ 222466.9 ($J = 4$)^o	9.94E + 08	1.55E + 08	− 2.35
466.074	$5s^25p^64f^2$ 5743.4 ($J = 6$)	$5s^25p^54f^25d$ 220304.1 ($J = 6$)^o	1.47E + 09	1.17E + 09	− 1.43
466.189	$5s^25p^64f^2$ 2834.3 ($J = 5$)	$5s^25p^54f^25d$ 217341.6 ($J = 4$)^o	9.77E + 08	2.10E + 09	− 1.24
466.401	$5s^25p^64f^2$ 8311.4 ($J = 4$)	$5s^25p^54f^25d$ 222716.4 ($J = 5$)^o	1.03E + 09	3.54E + 09	− 1.02
466.940	$5s^25p^64f^2$ 8311.4 ($J = 4$)	$5s^25p^54f^25d$ 222466.9 ($J = 4$)^o	1.49E + 09	2.30E + 09	− 1.18
466.976	$5s^25p^64f^2$ 12269.7 ($J = 4$)	$5s^25p^54f^25d$ 226411.4 ($J = 5$)^o	8.45E + 08	5.24E + 08	− 1.78
467.580	$5s^25p^64f^2$ 12269.7 ($J = 4$)	$5s^25p^54f^25d$ 226134.9 ($J = 3$)^o	2.83E + 09	9.87E + 08	− 1.53
467.825	$5s^25p^64f^2$ 7784.8 ($J = 3$)	$5s^25p^54f^25d$ 221538.1 ($J = 4$)^o	7.54E + 08	1.63E + 07	− 3.30
467.876	$5s^25p^64f^2$ 0.0 ($J = 4$)	$5s^25p^54f^25d$ 213738.5 ($J = 4$)^o	1.08E + 09	2.28E + 08	− 2.20
468.023	$5s^25p^64f^2$ 2834.3 ($J = 5$)	$5s^25p^54f^25d$ 216499.5 ($J = 5$)^o	2.19E + 09	1.07E + 09	− 1.46
468.101	$5s^25p^64f^2$ 7784.8 ($J = 3$)	$5s^25p^54f^25d$ 221416.7 ($J = 3$)^o	5.71E + 07	5.31E + 08	− 1.78
468.488	$5s^25p^64f^2$ 0.0 ($J = 4$)	$5s^25p^54f^25d$ 213453.0 ($J = 5$)^o	1.88E + 09	9.28E + 08	− 1.57
468.602	$5s^25p^64f^2$ 12269.7 ($J = 4$)	$5s^25p^54f^25d$ 225668.8 ($J = 5$)^o	1.40E + 09	2.02E + 08	− 2.14
468.921	$5s^25p^64f^2$ 7784.8 ($J = 3$)	$5s^25p^54f^25d$ 221040.4 ($J = 3$)^o	1.44E + 09	1.45E + 07	− 3.28

Table 6 – *continued*

λ_{obs} (Å)[a]	Transition		gA (s^{-1})		log gf
	Lower level	Upper level	Previous[a]	HFR + CPOL[b]	HFR + CPOL[b]
468.974	$5s^25p^64f^2$ 8311.4 ($J = 4$)	$5s^25p^54f^25d$ 221538.1 ($J = 4$)^o	4.30E + 09	3.54E + 06	− 3.96
469.504	$5s^25p^64f^2$ 2834.3 ($J = 5$)	$5s^25p^54f^25d$ 215828.5 ($J = 5$)^o	6.13E + 07	6.51E + 08	− 1.78
469.552	$5s^25p^64f^2$ 7784.8 ($J = 3$)	$5s^25p^54f^25d$ 220754.5 ($J = 4$)^o	7.25E + 08	1.55E + 08	− 2.35
469.711	$5s^25p^64f^2$ 5743.4 ($J = 6$)	$5s^25p^54f^25d$ 218638.7 ($J = 5$)^o	8.05E + 08	4.40E + 08	− 1.87
470.071	$5s^25p^64f^2$ 8311.4 ($J = 4$)	$5s^25p^54f^25d$ 221040.4 ($J = 3$)^o	7.30E + 06	1.59E + 07	− 2.42
470.146	$5s^25p^64f^2$ 26088.1 ($J = 6$)	$5s^25p^54f^25d$ 238787.0 ($J = 7$)^o	7.78E + 08	1.15E + 09	− 1.42
470.326	$5s^25p^64f^2$ 2834.3 ($J = 5$)	$5s^25p^54f^25d$ 215456.7 ($J = 5$)^o	2.28E + 09	1.07E + 09	− 1.46
470.350	$5s^25p^64f^2$ 5743.4 ($J = 6$)	$5s^25p^54f^25d$ 218353.2 ($J = 6$)^o	7.32E + 08	1.17E + 09	− 1.43
470.405	$5s^25p^64f^2$ 7784.8 ($J = 3$)	$5s^25p^54f^25d$ 220368.9 ($J = 3$)^o	9.91E + 08	1.22E + 08	− 2.44
471.122	$5s^25p^64f^2$ 12269.7 ($J = 4$)	$5s^25p^54f^25d$ 224529.3 ($J = 4$)^o	1.27E + 09	1.15E + 09	− 1.43
471.183	$5s^25p^64f^2$ 25892.9 ($J = 1$)	$5s^25p^54f^25d$ 238127.6 ($J = 2$)^o	9.39E + 08	4.08E + 08	− 2.05
471.353	$5s^25p^64f^2$ 8311.4 ($J = 4$)	$5s^25p^54f^25d$ 220472.9 ($J = 5$)^o	4.26E + 08	4.66E + 08	− 1.83
471.567	$5s^25p^64f^2$ 8311.4 ($J = 4$)	$5s^25p^54f^25d$ 220368.9 ($J = 3$)^o	2.67E + 09	2.79E + 08	− 2.08
471.916	$5s^25p^64f^2$ 7784.8 ($J = 3$)	$5s^25p^54f^25d$ 219685.7 ($J = 4$)^o	5.32E + 08	1.09E + 07	− 3.44
473.309	$5s^25p^64f^2$ 0.0 ($J = 4$)	$5s^25p^54f^25d$ 211278.3 ($J = 3$)^o	1.05E + 08	1.29E + 08	− 2.31
473.387	$5s^25p^64f^2$ 0.0 ($J = 4$)	$5s^25p^54f^25d$ 211247.3 ($J = 5$)^o	1.19E + 09	2.90E + 09	− 1.05
473.835	$5s^25p^64f^2$ 20551.4 ($J = 2$)	$5s^25p^54f^25d$ 231592.0 ($J = 3$)^o	2.85E + 08	2.41E + 08	− 2.13
473.969	$5s^25p^64f^2$ 12269.7 ($J = 4$)	$5s^25p^54f^25d$ 223252.1 ($J = 3$)^o	8.49E + 08	1.30E + 08	− 2.35
474.111	$5s^25p^64f^2$ 0.0 ($J = 4$)	$5s^25p^54f^25d$ 210920.2 ($J = 4$)^o	3.85E + 08	4.30E + 08	− 1.85
474.414	$5s^25p^64f^2$ 8311.4 ($J = 4$)	$5s^25p^54f^25d$ 219103.5 ($J = 5$)^o	1.83E + 08	3.83E + 08	− 1.90
474.861	$5s^25p^64f^2$ 2834.3 ($J = 5$)	$5s^25p^54f^25d$ 213423.3 ($J = 6$)^o	1.10E + 09	1.68E + 09	− 1.25
474.861	$5s^25p^64f^2$ 7784.8 ($J = 3$)	$5s^25p^54f^25d$ 218371.0 ($J = 4$)^o	4.11E + 08	1.63E + 07	− 3.30
474.953	$5s^25p^64f^2$ 0.0 ($J = 4$)	$5s^25p^54f^25d$ 210545.7 ($J = 5$)^o	2.60E + 08	9.28E + 08	− 1.57
475.445	$5s^25p^64f^2$ 12269.7 ($J = 4$)	$5s^25p^54f^25d$ 222602.3 ($J = 3$)^o	4.63E + 08	2.61E + 09	− 1.27
475.891	$5s^25p^64f^2$ 7784.8 ($J = 3$)	$5s^25p^54f^25d$ 217916.4 ($J = 4$)^o	5.74E + 08	1.54E + 09	− 1.32
475.984	$5s^25p^64f^2$ 5743.4 ($J = 6$)	$5s^25p^54f^25d$ 215828.5 ($J = 5$)^o	5.12E + 08	1.38E + 08	− 2.35
476.683	$5s^25p^64f^2$ 12269.7 ($J = 4$)	$5s^25p^54f^25d$ 222061.2 ($J = 5$)^o	9.37E + 08	6.24E + 08	− 1.67
477.870	$5s^25p^64f^2$ 12269.7 ($J = 4$)	$5s^25p^54f^25d$ 221538.1 ($J = 4$)^o	5.66E + 08	5.09E + 08	− 1.79
479.649	$5s^25p^64f^2$ 12269.7 ($J = 4$)	$5s^25p^54f^25d$ 220754.5 ($J = 4$)^o	1.04E + 08	3.64E + 08	− 1.96
479.817	$5s^25p^64f^2$ 2834.3 ($J = 5$)	$5s^25p^54f^25d$ 211247.3 ($J = 5$)^o	1.15E + 09	6.94E + 08	− 1.66
480.299	$5s^25p^64f^2$ 12269.7 ($J = 4$)	$5s^25p^54f^25d$ 220472.9 ($J = 5$)^o	1.99E + 07	2.11E + 08	− 2.16
480.445	$5s^25p^64f^2$ 0.0 ($J = 4$)	$5s^25p^54f^25d$ 208143.8 ($J = 5$)^o	5.30E + 08	2.90E + 09	− 1.05
480.569	$5s^25p^64f^2$ 2834.3 ($J = 5$)	$5s^25p^54f^25d$ 210920.2 ($J = 4$)^o	3.16E + 08	9.84E + 07	− 2.48
480.569	$5s^25p^64f^2$ 25892.9 ($J = 1$)	$5s^25p^54f^25d$ 233979.7 ($J = 2$)^o	1.01E + 08	8.84E + 07	− 2.52
480.740	$5s^25p^64f^2$ 26088.1 ($J = 6$)	$5s^25p^54f^25d$ 234105.4 ($J = 5$)^o	1.39E + 09	9.61E + 09	− 0.61
481.122	$5s^25p^64f^2$ 26088.1 ($J = 6$)	$5s^25p^54f^25d$ 233935.4 ($J = 7$)^o	1.34E + 09	3.36E + 09	− 0.98
481.435	$5s^25p^64f^2$ 2834.3 ($J = 5$)	$5s^25p^54f^25d$ 210545.7 ($J = 5$)^o	2.59E + 09	1.58E + 08	− 2.41
481.435	$5s^25p^64f^2$ 5743.4 ($J = 6$)	$5s^25p^54f^25d$ 213453.0 ($J = 5$)^o	8.60E + 08	1.95E + 08	− 2.22
481.509	$5s^25p^64f^2$ 5743.4 ($J = 6$)	$5s^25p^54f^25d$ 213423.3 ($J = 6$)^o	5.82E + 08	9.80E + 08	− 1.48
482.119	$5s^25p^64f^2$ 12269.7 ($J = 4$)	$5s^25p^54f^25d$ 219685.7 ($J = 4$)^o	7.15E + 08	2.23E + 08	− 2.12
482.741	$5s^25p^64f^2$ 0.0 ($J = 4$)	$5s^25p^54f^25d$ 207148.2 ($J = 5$)^o	2.14E + 09	1.07E + 08	− 2.45
482.741	$5s^25p^64f^2$ 8311.4 ($J = 4$)	$5s^25p^54f^25d$ 215456.7 ($J = 5$)^o	8.11E + 08	1.55E + 07	− 3.28
483.474	$5s^25p^64f^2$ 12269.7 ($J = 4$)	$5s^25p^54f^25d$ 219103.5 ($J = 5$)^o	2.76E + 08	1.54E + 08	− 2.33
484.244	$5s^25p^64f^2$ 0.0 ($J = 4$)	$5s^25p^54f^25d$ 206509.1 ($J = 5$)^o	6.46E + 08	2.13E + 08	− 2.14
484.577	$5s^25p^64f^2$ 12269.7 ($J = 4$)	$5s^25p^54f^25d$ 218638.7 ($J = 5$)^o	1.59E + 08	2.11E + 08	− 2.16
485.529	$5s^25p^64f^2$ 7784.8 ($J = 3$)	$5s^25p^54f^25d$ 213738.5 ($J = 4$)^o	3.76E + 08	1.56E + 08	− 2.34
486.050	$5s^25p^64f^2$ 0.0 ($J = 4$)	$5s^25p^54f^25d$ 205744.4 ($J = 4$)^o	2.01E + 08	6.19E + 07	− 2.64
486.795	$5s^25p^64f^2$ 8311.4 ($J = 4$)	$5s^25p^54f^25d$ 213738.5 ($J = 4$)^o	1.32E + 08	1.13E + 09	− 1.47
486.881	$5s^25p^64f^2$ 5893.8 ($J = 2$)	$5s^25p^54f^25d$ 211278.3 ($J = 3$)^o	2.35E + 08	3.28E + 08	− 1.93
487.468	$5s^25p^64f^2$ 8311.4 ($J = 4$)	$5s^25p^54f^25d$ 213453.0 ($J = 5$)^o	1.36E + 09	4.60E + 08	− 1.84
487.629	$5s^25p^64f^2$ 12269.7 ($J = 4$)	$5s^25p^54f^25d$ 217341.6 ($J = 4$)^o	4.85E + 08	7.28E + 07	− 2.57
488.281	$5s^25p^64f^2$ 5743.4 ($J = 6$)	$5s^25p^54f^25d$ 210545.7 ($J = 5$)^o	9.57E + 07	1.95E + 08	− 2.22
490.971	$5s^25p^64f^2$ 2834.3 ($J = 5$)	$5s^25p^54f^25d$ 206509.1 ($J = 5$)^o	4.98E + 08	1.18E + 08	− 2.40
491.084	$5s^25p^64f^2$ 20551.4 ($J = 2$)	$5s^25p^54f^25d$ 224181.2 ($J = 2$)^o	2.21E + 08	1.92E + 08	− 2.16
491.169	$5s^25p^64f^2$ 0.0 ($J = 4$)	$5s^25p^54f^25d$ 203596.3 ($J = 5$)^o	1.94E + 08	2.28E + 07	− 3.09
491.279	$5s^25p^64f^2$ 12269.7 ($J = 4$)	$5s^25p^54f^25d$ 215828.5 ($J = 5$)^o	4.26E + 08	1.93E + 08	− 2.17
491.422	$5s^25p^64f^2$ 7784.8 ($J = 3$)	$5s^25p^54f^25d$ 211278.3 ($J = 3$)^o	1.16E + 08	1.23E + 07	− 3.25
491.730	$5s^25p^64f^2$ 20551.4 ($J = 2$)	$5s^25p^54f^25d$ 223914.6 ($J = 3$)^o	4.31E + 08	1.83E + 08	− 2.24
492.158	$5s^25p^64f^2$ 12269.7 ($J = 4$)	$5s^25p^54f^25d$ 215456.7 ($J = 5$)^o	1.23E + 08	3.93E + 07	− 2.86
492.695	$5s^25p^64f^2$ 8311.4 ($J = 4$)	$5s^25p^54f^25d$ 211278.3 ($J = 3$)^o	4.77E + 08	4.76E + 07	− 2.77
492.769	$5s^25p^64f^2$ 8311.4 ($J = 4$)	$5s^25p^54f^25d$ 211247.3 ($J = 5$)^o	2.72E + 08	4.99E + 08	− 1.78
492.830	$5s^25p^64f^2$ 2834.3 ($J = 5$)	$5s^25p^54f^25d$ 205744.4 ($J = 4$)^o	2.18E + 09	3.50E + 08	− 1.91
493.343	$5s^25p^64f^2$ 20551.4 ($J = 2$)	$5s^25p^54f^25d$ 223252.7 ($J = 3$)^o	1.67E + 08	5.67E + 07	− 2.69
493.571	$5s^25p^64f^2$ 8311.4 ($J = 4$)	$5s^25p^54f^25d$ 210920.2 ($J = 4$)^o	1.40E + 08	1.70E + 08	− 2.23

Table 6 – *continued*

λ_{obs} (Å)[a]	Transition		gA (s^{-1})		log gf
	Lower level	Upper level	Previous[a]	HFR + CPOL[b]	HFR + CPOL[b]
494.061	$5s^25p^64f^2$ 5743.4 ($J = 6$)	$5s^25p^54f^25d$ 208143.8 ($J = 5$)^o	6.28E + 08	1.45E + 08	− 2.33
496.355	$5s^25p^64f^2$ 12269.7 ($J = 4$)	$5s^25p^54f^25d$ 213738.5 ($J = 4$)^o	8.55E + 08	5.64E + 08	− 1.75
496.512	$5s^25p^64f^2$ 5743.4 ($J = 6$)	$5s^25p^54f^25d$ 207148.2 ($J = 5$)^o	3.53E + 08	3.77E + 07	− 2.87
497.838	$5s^25p^64f^2$ 20551.4 ($J = 2$)	$5s^25p^54f^25d$ 221416.7 ($J = 3$)^o	9.50E + 07	8.49E + 07	− 2.51
498.098	$5s^25p^64f^2$ 5743.4 ($J = 6$)	$5s^25p^54f^25d$ 206509.1 ($J = 5$)^o	5.88E + 08	4.68E + 08	− 1.79
498.232	$5s^25p^64f^2$ 27478.7 ($J = 2$)	$5s^25p^54f^25d$ 228189.8 ($J = 3$)^o	1.35E + 08	2.62E + 08	− 2.02
498.685	$5s^25p^64f^2$ 26088.1 ($J = 6$)	$5s^25p^54f^25d$ 226618.2 ($J = 5$)^o	2.00E + 08	2.38E + 07	− 3.05
499.177	$5s^25p^64f^2$ 0.0 ($J = 4$)	$5s^25p^54f^25d$ 200327.2 ($J = 4$)^o	1.43E + 08	3.60E + 08	− 1.89
499.546	$5s^25p^64f^2$ 26088.1 ($J = 6$)	$5s^25p^54f^25d$ 226271.3 ($J = 7$)^o	2.34E + 08	2.05E + 10	− 0.21
499.872	$5s^25p^64f^2$ 2834.3 ($J = 5$)	$5s^25p^54f^25d$ 202884.9 ($J = 6$)^o	3.65E + 08	9.33E + 07	− 2.47
500.421	$5s^25p^64f^2$ 8311.4 ($J = 4$)	$5s^25p^54f^25d$ 208143.8 ($J = 5$)^o	3.52E + 08	4.99E + 08	− 1.78
502.495	$5s^25p^64f^2$ 12269.7 ($J = 4$)	$5s^25p^54f^25d$ 211278.3 ($J = 3$)^o	3.73E + 08	1.78E + 08	− 2.17
502.559	$5s^25p^64f^2$ 12269.7 ($J = 4$)	$5s^25p^54f^25d$ 211247.3 ($J = 5$)^o	1.89E + 08	2.67E + 08	− 2.01
503.093	$5s^25p^64f^2$ 2834.3 ($J = 5$)	$5s^25p^54f^25d$ 201606.0 ($J = 5$)^o	2.62E + 08	2.59E + 09	− 1.11
503.384	$5s^25p^64f^2$ 27478.7 ($J = 2$)	$5s^25p^54f^25d$ 226134.9 ($J = 3$)^o	1.58E + 09	3.68E + 08	− 2.02
504.091	$5s^25p^64f^2$ 26088.1 ($J = 6$)	$5s^25p^54f^25d$ 224461.6 ($J = 6$)^o	8.51E + 07	7.80E + 08	− 1.55
504.547	$5s^25p^64f^2$ 8311.4 ($J = 4$)	$5s^25p^54f^25d$ 206509.1 ($J = 5$)^o	1.98E + 08	6.24E + 08	− 1.79
505.148	$5s^25p^64f^2$ 7784.8 ($J = 3$)	$5s^25p^54f^25d$ 205744.4 ($J = 4$)^o	1.63E + 08	4.79E + 06	− 3.74
505.425	$5s^25p^64f^2$ 5743.4 ($J = 6$)	$5s^25p^54f^25d$ 203596.3 ($J = 5$)^o	1.25E + 09	3.39E + 08	− 1.89
507.251	$5s^25p^64f^2$ 5743.4 ($J = 6$)	$5s^25p^54f^25d$ 202884.9 ($J = 6$)^o	5.01E + 08	4.92E + 08	− 1.72
507.919	$5s^25p^64f^2$ 25892.9 ($J = 1$)	$5s^25p^54f^25d$ 222773.5 ($J = 2$)^o	1.65E + 08	6.85E + 05	− 4.52
508.392	$5s^25p^64f^2$ 27478.7 ($J = 2$)	$5s^25p^54f^25d$ 224181.2 ($J = 2$)^o	4.19E + 08	6.86E + 05	− 4.52
508.568	$5s^25p^64f^2$ 26088.1 ($J = 6$)	$5s^25p^54f^25d$ 222716.4 ($J = 5$)^o	2.13E + 08	6.08E + 06	− 3.62
510.267	$5s^25p^64f^2$ 26088.1 ($J = 6$)	$5s^25p^54f^25d$ 222061.2 ($J = 5$)^o	5.20E + 08	1.21E + 08	− 2.32
513.634	$5s^25p^64f^2$ 5893.8 ($J = 2$)	$5s^25p^54f^25d$ 200585.8 ($J = 3$)^o	1.92E + 08	9.04E + 06	− 3.43
514.828	$5s^25p^64f^2$ 12269.7 ($J = 4$)	$5s^25p^54f^25d$ 206509.1 ($J = 5$)^o	1.09E + 08	5.91E + 07	− 2.61
514.887	$5s^25p^64f^2$ 26088.1 ($J = 6$)	$5s^25p^54f^25d$ 220304.1 ($J = 6$)^o	3.95E + 08	1.56E + 08	− 2.18
515.326	$5s^25p^64f^2$ 7784.8 ($J = 3$)	$5s^25p^54f^25d$ 201838.5 ($J = 4$)^o	1.07E + 08	2.92E + 08	− 1.97
516.056	$5s^25p^64f^2$ 5893.8 ($J = 2$)	$5s^25p^54f^25d$ 199673.6 ($J = 1$)^o	2.29E + 08	3.26E + 08	− 1.89
516.720	$5s^25p^64f^2$ 8311.4 ($J = 4$)	$5s^25p^54f^25d$ 201838.5 ($J = 4$)^o	7.06E + 07	2.55E + 07	− 3.00
516.859	$5s^25p^64f^2$ 12269.7 ($J = 4$)	$5s^25p^54f^25d$ 205744.4 ($J = 4$)^o	3.88E + 08	7.63E + 07	− 2.51
518.668	$5s^25p^64f^2$ 7784.8 ($J = 3$)	$5s^25p^54f^25d$ 200585.8 ($J = 3$)^o	2.09E + 08	8.69E + 07	− 2.44
520.115	$5s^25p^64f^2$ 26088.1 ($J = 6$)	$5s^25p^54f^25d$ 218353.2 ($J = 6$)^o	5.26E + 08	1.56E + 08	− 2.18
520.797	$5s^25p^64f^2$ 8311.4 ($J = 4$)	$5s^25p^54f^25d$ 200327.2 ($J = 4$)^o	9.02E + 07	6.95E + 07	− 2.56
527.512	$5s^25p^64f^2$ 12269.7 ($J = 4$)	$5s^25p^54f^25d$ 201838.5 ($J = 4$)^o	7.37E + 07	1.11E + 07	− 3.37
528.159	$5s^25p^64f^2$ 12269.7 ($J = 4$)	$5s^25p^54f^25d$ 201606.0 ($J = 5$)^o	1.07E + 08	5.83E + 08	− 1.72
544.068	$5s^25p^64f^2$ 27478.7 ($J = 2$)	$5s^25p^54f^25d$ 211278.3 ($J = 3$)^o	2.58E + 08	3.38E + 07	− 2.81
552.305	$5s^25p^64f^2$ 26088.1 ($J = 6$)	$5s^25p^54f^25d$ 207148.2 ($J = 5$)^o	1.52E + 08	5.76E + 06	− 3.59
575.433	$5s^25p^64f^2$ 25892.9 ($J = 1$)	$5s^25p^54f^25d$ 199673.6 ($J = 1$)^o	1.27E + 08	5.24E + 07	− 2.58
713.891	$5s^25p^64f^2$ 2834.3 ($J = 5$)	$5s^25p^64f5d$ 142910.8 ($J = 5$)^o	5.00E + 06	2.51E + 06	− 3.68
729.036	$5s^25p^64f^2$ 5743.4 ($J = 6$)	$5s^25p^64f5d$ 142910.8 ($J = 5$)^o	6.20E + 07	6.07E + 07	− 2.28
738.999	$5s^25p^64f^2$ 0.0 ($J = 4$)	$5s^25p^64f5d$ 135318.3 ($J = 3$)^o	3.20E + 07	2.85E + 07	− 2.60
742.942	$5s^25p^64f^2$ 8311.4 ($J = 4$)	$5s^25p^64f5d$ 142910.8 ($J = 5$)^o	3.20E + 07	6.90E + 07	− 2.21
744.269	$5s^25p^64f^2$ 0.0 ($J = 4$)	$5s^25p^64f5d$ 134359.7 ($J = 4$)^o	2.00E + 07	2.91E + 07	− 2.58
748.900	$5s^25p^64f^2$ 2834.3 ($J = 5$)	$5s^25p^64f5d$ 136363.4 ($J = 6$)^o	3.00E + 07	4.26E + 07	− 2.42
754.159	$5s^25p^64f^2$ 0.0 ($J = 4$)	$5s^25p^64f5d$ 132597.5 ($J = 5$)^o	3.00E + 07	4.27E + 07	− 2.41
756.472	$5s^25p^64f^2$ 2834.3 ($J = 5$)	$5s^25p^64f5d$ 135027.2 ($J = 5$)^o	9.80E + 07	1.19E + 08	− 1.95
756.650	$5s^25p^64f^2$ 0.0 ($J = 4$)	$5s^25p^64f5d$ 132162.1 ($J = 4$)^o	9.10E + 07	1.44E + 08	− 1.87
758.925	$5s^25p^64f^2$ 7784.8 ($J = 3$)	$5s^25p^64f5d$ 139549.8 ($J = 3$)^o	2.40E + 07	4.62E + 07	− 2.36
760.311	$5s^25p^64f^2$ 2834.3 ($J = 5$)	$5s^25p^64f5d$ 134359.7 ($J = 4$)^o	1.42E + 08	1.09E + 08	− 1.99
761.971	$5s^25p^64f^2$ 8311.4 ($J = 4$)	$5s^25p^64f5d$ 139549.8 ($J = 3$)^o	1.80E + 07	4.80E + 07	− 2.34
762.753	$5s^25p^64f^2$ 0.0 ($J = 4$)	$5s^25p^64f5d$ 131104.7 ($J = 3$)^o	1.53E + 08	1.23E + 08	− 1.93
765.456	$5s^25p^64f^2$ 12269.7 ($J = 4$)	$5s^25p^64f5d$ 142910.8 ($J = 5$)^o	1.86E + 08	1.82E + 08	− 1.76
765.579	$5s^25p^64f^2$ 5743.4 ($J = 6$)	$5s^25p^64f5d$ 136363.4 ($J = 6$)^o	9.35E + 08	1.34E + 09	− 0.90
765.973	$5s^25p^64f^2$ 0.0 ($J = 4$)	$5s^25p^64f5d$ 130553.0 ($J = 4$)^o	2.39E + 08	3.88E + 08	− 1.43
770.635	$5s^25p^64f^2$ 2834.3 ($J = 5$)	$5s^25p^64f5d$ 132597.5 ($J = 5$)^o	7.88E + 08	1.14E + 09	− 0.96
773.230	$5s^25p^64f^2$ 2834.3 ($J = 5$)	$5s^25p^64f5d$ 132162.1 ($J = 4$)^o	3.23E + 10	4.31E + 09	− 0.37
773.493	$5s^25p^64f^2$ 5743.4 ($J = 6$)	$5s^25p^64f5d$ 135027.2 ($J = 5$)^o	4.08E + 10	5.47E + 09	− 0.27
774.567	$5s^25p^64f^2$ 0.0 ($J = 4$)	$5s^25p^64f5d$ 129104.5 ($J = 3$)^o	2.51E + 10	3.48E + 09	− 0.46
783.863	$5s^25p^64f^2$ 7784.8 ($J = 3$)	$5s^25p^64f5d$ 135359.2 ($J = 2$)^o	9.13E + 08	1.14E + 09	− 0.94
783.912	$5s^25p^64f^2$ 0.0 ($J = 4$)	$5s^25p^64f5d$ 127565.1 ($J = 4$)^o	4.13E + 08	5.32E + 08	− 1.27
784.105	$5s^25p^64f^2$ 7784.8 ($J = 3$)	$5s^25p^64f5d$ 135318.3 ($J = 3$)^o	8.10E + 07	1.39E + 08	− 1.85
784.483	$5s^25p^64f^2$ 5893.8 ($J = 2$)	$5s^25p^64f5d$ 133366.3 ($J = 1$)^o	6.97E + 08	9.74E + 08	− 1.01
785.669	$5s^25p^64f^2$ 12269.7 ($J = 4$)	$5s^25p^64f5d$ 139549.8 ($J = 3$)^o	2.03E + 09	2.66E + 09	− 0.57

Table 6 – *continued*

λ_{obs} (Å)[a]	Transition		gA (s^{-1})		log gf
	Lower level	Upper level	Previous[a]	HFR + CPOL[b]	HFR + CPOL[b]
787.091	$5s^25p^64f^2$ 20551.4 ($J = 2$)	$5s^25p^64f5d$ 147601.4 ($J = 1$)^o	4.66E + 08	6.27E + 08	− 1.18
787.359	$5s^25p^64f^2$ 8311.4 ($J = 4$)	$5s^25p^64f5d$ 135318.3 ($J = 3$)^o	1.74E + 09	2.46E + 09	− 0.60
789.169	$5s^25p^64f^2$ 8311.4 ($J = 4$)	$5s^25p^64f5d$ 135027.2 ($J = 5$)^o	2.60E + 08	2.55E + 08	− 1.58
789.440	$5s^25p^64f^2$ 5893.8 ($J = 2$)	$5s^25p^64f5d$ 132565.8 ($J = 2$)^o	6.80E + 07	2.57E + 07	− 2.58
790.043	$5s^25p^64f^2$ 7784.8 ($J = 3$)	$5s^25p^64f5d$ 134359.7 ($J = 4$)^o	3.20E + 07	5.62E + 07	− 2.24
793.348	$5s^25p^64f^2$ 8311.4 ($J = 4$)	$5s^25p^64f5d$ 134359.7 ($J = 4$)^o	3.94E + 08	2.73E + 08	− 1.55
798.654	$5s^25p^64f^2$ 5893.8 ($J = 2$)	$5s^25p^64f5d$ 131104.7 ($J = 3$)^o	3.90E + 07	6.97E + 07	− 2.13
801.406	$5s^25p^64f^2$ 7784.8 ($J = 3$)	$5s^25p^64f5d$ 132565.8 ($J = 2$)^o	2.17E + 08	4.07E + 08	− 1.37
804.005	$5s^25p^64f^2$ 7784.8 ($J = 3$)	$5s^25p^64f5d$ 132162.1 ($J = 4$)^o	2.94E + 08	3.58E + 08	− 1.41
810.898	$5s^25p^64f^2$ 7784.8 ($J = 3$)	$5s^25p^64f5d$ 131104.7 ($J = 3$)^o	9.94E + 08	1.32E + 09	− 0.84
811.616	$5s^25p^64f^2$ 5893.8 ($J = 2$)	$5s^25p^64f5d$ 129104.5 ($J = 3$)^o	2.29E + 08	2.66E + 08	− 1.53
814.378	$5s^25p^64f^2$ 8311.4 ($J = 4$)	$5s^25p^64f5d$ 131104.7 ($J = 3$)^o	6.10E + 07	1.27E + 08	− 1.85
814.539	$5s^25p^64f^2$ 7784.8 ($J = 3$)	$5s^25p^64f5d$ 130553.0 ($J = 4$)^o	1.30E + 07	6.74E + 06	− 3.13
814.616	$5s^25p^64f^2$ 12269.7 ($J = 4$)	$5s^25p^64f5d$ 135027.2 ($J = 5$)^o	7.10E + 07	2.55E + 08	− 1.58
815.987	$5s^25p^64f^2$ 25050.6 ($J = 0$)	$5s^25p^64f5d$ 147601.4 ($J = 1$)^o	1.90E + 07	2.73E + 07	− 2.51
817.297	$5s^25p^64f5d$ 127565.1 ($J = 4$)^o	$5s^25p^64f6p$ 249919.6 ($J = 4$)	9.57E + 08	1.34E + 09	− 0.89
818.060	$5s^25p^64f^2$ 8311.4 ($J = 4$)	$5s^25p^64f5d$ 130553.0 ($J = 4$)^o	4.90E + 08	6.27E + 08	− 1.16
819.065	$5s^25p^64f^2$ 12269.7 ($J = 4$)	$5s^25p^64f5d$ 134359.7 ($J = 4$)^o	8.96E + 08	1.47E + 09	− 0.79
821.930	$5s^25p^64f^2$ 5893.8 ($J = 2$)	$5s^25p^64f5d$ 127558.8 ($J = 2$)^o	6.51E + 08	9.56E + 08	− 0.97
827.858	$5s^25p^64f^2$ 8311.4 ($J = 4$)	$5s^25p^64f5d$ 129104.5 ($J = 3$)^o	1.90E + 07	1.82E + 07	− 2.68
830.152	$5s^25p^64f5d$ 131104.7 ($J = 3$)^o	$5s^25p^64f6p$ 251563.0 ($J = 2$)	6.46E + 08	7.60E + 08	− 1.13
832.481	$5s^25p^64f^2$ 27478.7 ($J = 2$)	$5s^25p^64f5d$ 147601.4 ($J = 1$)^o	1.25E + 08	1.70E + 08	− 1.69
834.082	$5s^25p^64f^2$ 12269.7 ($J = 4$)	$5s^25p^64f5d$ 132162.1 ($J = 4$)^o	3.00E + 06	8.80E + 04	− 5.00
834.912	$5s^25p^64f^2$ 7784.8 ($J = 3$)	$5s^25p^64f5d$ 127558.8 ($J = 2$)^o	1.30E + 07	3.14E + 07	− 2.44
836.311	$5s^25p^64f5d$ 127558.8 ($J = 2$)^o	$5s^25p^64f6p$ 247130.7 ($J = 1$)	1.35E + 09	1.82E + 09	− 0.74
838.547	$5s^25p^64f^2$ 8311.4 ($J = 4$)	$5s^25p^64f5d$ 127565.1 ($J = 4$)^o	3.22E + 08	6.47E + 08	− 1.12
839.543	$5s^25p^64f5d$ 127565.1 ($J = 4$)^o	$5s^25p^64f6p$ 246677.6 ($J = 4$)	4.06E + 09	4.97E + 09	− 0.30
840.350	$5s^25p^64f^2$ 20551.4 ($J = 2$)	$5s^25p^64f5d$ 139549.8 ($J = 3$)^o	9.80E + 07	8.10E + 07	− 2.00
840.350	$5s^25p^64f5d$ 132565.8 ($J = 2$)^o	$5s^25p^64f6p$ 251563.0 ($J = 2$)	2.44E + 09	1.99E + 09	− 0.69
845.426	$5s^25p^64f^2$ 12269.7 ($J = 4$)	$5s^25p^64f5d$ 130553.0 ($J = 4$)^o	5.50E + 07	7.30E + 06	− 3.07
848.507	$5s^25p^64f5d$ 132162.1 ($J = 4$)^o	$5s^25p^64f6p$ 250015.7 ($J = 5$)	6.59E + 08	7.85E + 08	− 1.10
849.200	$5s^25p^64f5d$ 132162.1 ($J = 4$)^o	$5s^25p^64f6p$ 249919.6 ($J = 4$)	6.26E + 08	2.27E + 08	− 1.63
849.444	$5s^25p^64f^2$ 20551.4 ($J = 2$)	$5s^25p^64f5d$ 138275.4 ($J = 1$)^o	1.18E + 08	1.70E + 08	− 1.68
851.653	$5s^25p^64f5d$ 132597.5 ($J = 5$)^o	$5s^25p^64f6p$ 250015.7 ($J = 5$)	1.44E + 09	1.75E + 09	− 0.74
855.995	$5s^25p^64f^2$ 26088.1 ($J = 6$)	$5s^25p^64f5d$ 142910.8 ($J = 5$)^o	4.36E + 09	6.20E + 09	− 0.11
860.561	$5s^25p^64f5d$ 135359.2 ($J = 2$)^o	$5s^25p^64f6p$ 251563.0 ($J = 2$)	2.34E + 09	3.53E + 09	− 0.42
861.143	$5s^25p^64f5d$ 130553.0 ($J = 4$)^o	$5s^25p^64f6p$ 246677.6 ($J = 4$)	5.48E + 08	4.26E + 08	− 1.34
864.631	$5s^25p^64f5d$ 134359.7 ($J = 4$)^o	$5s^25p^64f6p$ 250015.7 ($J = 5$)	9.41E + 08	9.52E + 08	− 0.99
865.353	$5s^25p^64f5d$ 134359.7 ($J = 4$)^o	$5s^25p^64f6p$ 249919.6 ($J = 4$)	6.93E + 09	7.85E + 09	− 0.07
866.776	$5s^25p^64f5d$ 134359.7 ($J = 4$)^o	$5s^25p^64f6p$ 249730.1 ($J = 3$)	7.53E + 09	8.30E + 09	− 0.05
867.342	$5s^25p^64f^2$ 12269.7 ($J = 4$)	$5s^25p^64f5d$ 127565.1 ($J = 4$)^o	1.06E + 08	9.35E + 07	− 1.93
867.622	$5s^25p^64f5d$ 131104.7 ($J = 3$)^o	$5s^25p^64f6p$ 246362.2 ($J = 2$)	4.42E + 09	4.87E + 09	− 0.28
868.546	$5s^25p^64f5d$ 127558.8 ($J = 2$)^o	$5s^25p^64f6p$ 242694.9 ($J = 3$)	5.40E + 07	1.90E + 08	− 1.69
868.584	$5s^25p^64f5d$ 127565.1 ($J = 4$)^o	$5s^25p^64f6p$ 242694.9 ($J = 3$)	6.63E + 08	7.17E + 08	− 1.12
869.650	$5s^25p^64f5d$ 135027.2 ($J = 5$)^o	$5s^25p^64f6p$ 250015.7 ($J = 5$)	6.92E + 09	8.37E + 09	− 0.05
870.381	$5s^25p^64f5d$ 135027.2 ($J = 5$)^o	$5s^25p^64f6p$ 249919.6 ($J = 4$)	3.31E + 09	3.31E + 09	− 0.45
871.020	$5s^25p^64f^2$ 20551.4 ($J = 2$)	$5s^25p^64f5d$ 135359.2 ($J = 2$)^o	6.40E + 07	1.58E + 08	− 1.69
871.333	$5s^25p^64f^2$ 20551.4 ($J = 2$)	$5s^25p^64f5d$ 135318.3 ($J = 3$)^o	2.35E + 08	3.28E + 08	− 1.36
872.339	$5s^25p^64f5d$ 130553.0 ($J = 4$)^o	$5s^25p^64f6p$ 245187.5 ($J = 3$)	9.03E + 09	1.75E + 08	− 1.70
872.869	$5s^25p^64f5d$ 132565.8 ($J = 2$)^o	$5s^25p^64f6p$ 247130.7 ($J = 1$)	1.48E + 09	1.55E + 09	− 0.77
873.241	$5s^25p^64f5d$ 132162.1 ($J = 4$)^o	$5s^25p^64f6p$ 246677.6 ($J = 4$)	9.59E + 08	1.18E + 09	− 0.89
874.034	$5s^25p^64f5d$ 135318.3 ($J = 3$)^o	$5s^25p^64f6p$ 249730.1 ($J = 3$)	9.75E + 08	8.67E + 08	− 1.02
874.981	$5s^25p^64f^2$ 25892.9 ($J = 1$)	$5s^25p^64f5d$ 140180.8 ($J = 2$)^o	1.78E + 08	2.74E + 08	− 1.44
876.574	$5s^25p^64f5d$ 132597.5 ($J = 5$)^o	$5s^25p^64f6p$ 246677.6 ($J = 4$)	9.24E + 09	1.10E + 10	0.09
878.758	$5s^25p^64f5d$ 132565.8 ($J = 2$)^o	$5s^25p^64f6p$ 246362.2 ($J = 2$)	3.75E + 09	5.00E + 09	− 0.25
879.009	$5s^25p^64f5d$ 133366.3 ($J = 1$)^o	$5s^25p^64f6p$ 247130.7 ($J = 1$)	2.05E + 09	2.60E + 09	− 0.54
879.876	$5s^25p^64f5d$ 136363.4 ($J = 6$)^o	$5s^25p^64f6p$ 250015.7 ($J = 5$)	2.45E + 10	2.73E + 10	0.49
880.359	$5s^25p^64f5d$ 129104.5 ($J = 3$)^o	$5s^25p^64f6p$ 242694.9 ($J = 3$)	6.40E + 08	4.83E + 08	− 1.28
883.204	$5s^25p^64f^2$ 25050.6 ($J = 0$)	$5s^25p^64f5d$ 138275.4 ($J = 1$)^o	1.42E + 08	2.11E + 08	− 1.55
884.759	$5s^25p^64f5d$ 132162.1 ($J = 4$)^o	$5s^25p^64f6p$ 245187.5 ($J = 3$)	4.84E + 09	7.25E + 09	− 0.08
884.982	$5s^25p^64f5d$ 133366.3 ($J = 1$)^o	$5s^25p^64f6p$ 246362.2 ($J = 2$)	1.19E + 08	2.20E + 08	− 1.60
887.294	$5s^25p^64f^2$ 27478.7 ($J = 2$)	$5s^25p^64f5d$ 140180.8 ($J = 2$)^o	8.18E + 08	1.12E + 09	− 0.82
887.899	$5s^25p^64f^2$ 25892.9 ($J = 1$)	$5s^25p^64f5d$ 138519.2 ($J = 0$)^o	2.05E + 08	2.84E + 08	− 1.41
888.619	$5s^25p^64f5d$ 130553.0 ($J = 4$)^o	$5s^25p^64f6p$ 243087.0 ($J = 4$)	2.81E + 09	2.26E + 09	− 0.60
889.820	$5s^25p^64f^2$ 25892.9 ($J = 1$)	$5s^25p^64f5d$ 138275.4 ($J = 1$)^o	1.85E + 08	2.45E + 08	− 1.47

Table 6 – *continued*

λ_{obs} (Å)[a]	Transition		gA (s^{-1})		log gf
	Lower level	Upper level	Previous[a]	HFR + CPOL[b]	HFR + CPOL[b]
890.329	$5s^25p^64f5d$ 134359.7 ($J = 4$)^o	$5s^25p^64f6p$ 246677.6 ($J = 4$)	1.64E + 09	1.18E + 09	− 0.89
891.732	$5s^25p^64f5d$ 130553.0 ($J = 4$)^o	$5s^25p^64f6p$ 242694.9 ($J = 3$)	1.76E + 09	1.75E + 08	− 1.70
892.292	$5s^25p^64f^2$ 27478.7 ($J = 2$)	$5s^25p^64f5d$ 139549.8 ($J = 3$)^o	2.59E + 08	3.74E + 08	− 1.28
892.743	$5s^25p^64f^2$ 20551.4 ($J = 2$)	$5s^25p^64f5d$ 132565.8 ($J = 2$)^o	5.60E + 08	7.83E + 08	− 0.97
892.743	$5s^25p^64f5d$ 139549.8 ($J = 3$)^o	$5s^25p^64f6p$ 251563.0 ($J = 2$)	2.92E + 09	3.26E + 09	− 0.43
892.998	$5s^25p^64f5d$ 131104.7 ($J = 3$)^o	$5s^25p^64f6p$ 243087.0 ($J = 4$)	1.21E + 09	1.27E + 09	− 0.85
895.464	$5s^25p^64f5d$ 127558.8 ($J = 2$)^o	$5s^25p^64f6p$ 239232.5 ($J = 2$)	5.56E + 09	6.35E + 09	− 0.14
895.662	$5s^25p^64f5d$ 135027.2 ($J = 5$)^o	$5s^25p^64f6p$ 246677.6 ($J = 4$)	6.97E + 09	7.94E + 09	− 0.04
896.137	$5s^25p^64f5d$ 131104.7 ($J = 3$)^o	$5s^25p^64f6p$ 242694.9 ($J = 3$)	3.61E + 09	5.36E + 09	− 0.22
897.818	$5s^25p^64f5d$ 140180.8 ($J = 2$)^o	$5s^25p^64f6p$ 251563.0 ($J = 2$)	1.80E + 09	1.95E + 09	− 0.64
897.992	$5s^25p^64f5d$ 135318.3 ($J = 3$)^o	$5s^25p^64f6p$ 246677.6 ($J = 4$)	9.62E + 08	9.36E + 08	− 0.96
899.852	$5s^25p^64f5d$ 127558.8 ($J = 2$)^o	$5s^25p^64f6p$ 238688.0 ($J = 3$)	1.75E + 09	1.87E + 09	− 0.67
899.905	$5s^25p^64f5d$ 127565.1 ($J = 4$)^o	$5s^25p^64f6p$ 238688.0 ($J = 3$)	1.06E + 10	1.10E + 10	0.10
900.548	$5s^25p^64f5d$ 135318.3 ($J = 3$)^o	$5s^25p^64f6p$ 246362.2 ($J = 2$)	1.75E + 09	1.96E + 09	− 0.64
900.876	$5s^25p^64f5d$ 135359.2 ($J = 2$)^o	$5s^25p^64f6p$ 246362.2 ($J = 2$)	1.37E + 09	1.10E + 09	− 0.89
901.521	$5s^25p^64f5d$ 132162.1 ($J = 4$)^o	$5s^25p^64f6p$ 243087.0 ($J = 4$)	4.87E + 09	6.75E + 09	− 0.12
902.557	$5s^25p^64f^2$ 27478.7 ($J = 2$)	$5s^25p^64f5d$ 138275.4 ($J = 1$)^o	1.65E + 08	2.24E + 08	− 1.50
904.708	$5s^25p^64f5d$ 132162.1 ($J = 4$)^o	$5s^25p^64f6p$ 242694.9 ($J = 3$)	3.97E + 09	7.25E + 09	− 0.08
905.068	$5s^25p^64f5d$ 132597.5 ($J = 5$)^o	$5s^25p^64f6p$ 243087.0 ($J = 4$)	9.38E + 09	9.79E + 09	0.06
906.045	$5s^25p^64f5d$ 139549.8 ($J = 3$)^o	$5s^25p^64f6p$ 249919.6 ($J = 4$)	1.87E + 09	2.27E + 09	− 0.57
907.601	$5s^25p^64f5d$ 139549.8 ($J = 3$)^o	$5s^25p^64f6p$ 249730.1 ($J = 3$)	6.37E + 09	8.07E + 09	− 0.02
908.034	$5s^25p^64f5d$ 132565.8 ($J = 2$)^o	$5s^25p^64f6p$ 242694.9 ($J = 3$)	5.57E + 08	1.16E + 08	− 1.87
908.034	$5s^25p^64f5d$ 129104.5 ($J = 3$)^o	$5s^25p^64f6p$ 239232.5 ($J = 2$)	4.93E + 09	6.10E + 09	− 0.15
910.176	$5s^25p^64f5d$ 135318.3 ($J = 3$)^o	$5s^25p^64f6p$ 245187.5 ($J = 3$)	2.55E + 09	2.66E + 09	− 0.49
912.542	$5s^25p^64f5d$ 129104.5 ($J = 3$)^o	$5s^25p^64f6p$ 238688.0 ($J = 3$)	4.97E + 09	6.08E + 09	− 0.15
912.837	$5s^25p^64f5d$ 140180.8 ($J = 2$)^o	$5s^25p^64f6p$ 249730.1 ($J = 3$)	4.78E + 09	5.98E + 09	− 0.14
913.522	$5s^25p^64f^2$ 25892.9 ($J = 1$)	$5s^25p^64f5d$ 135359.2 ($J = 2$)^o	2.97E + 08	3.57E + 08	− 1.28
917.947	$5s^25p^64f^2$ 26088.1 ($J = 6$)	$5s^25p^64f5d$ 135027.2 ($J = 5$)^o	6.30E + 07	7.45E + 07	− 1.96
918.653	$5s^25p^64f5d$ 138275.4 ($J = 1$)^o	$5s^25p^64f6p$ 247130.7 ($J = 1$)	1.93E + 09	2.11E + 09	− 0.59
919.732	$5s^25p^64f5d$ 134359.7 ($J = 4$)^o	$5s^25p^64f6p$ 243087.0 ($J = 4$)	2.85E + 08	6.80E + 08	− 1.09
920.719	$5s^25p^64f5d$ 138519.2 ($J = 0$)^o	$5s^25p^64f6p$ 247130.7 ($J = 1$)	1.65E + 09	1.93E + 09	− 0.63
921.212	$5s^25p^64f^2$ 20551.4 ($J = 2$)	$5s^25p^64f5d$ 129104.5 ($J = 3$)^o	6.00E + 06	9.09E + 06	− 2.86
923.053	$5s^25p^64f5d$ 134359.7 ($J = 4$)^o	$5s^25p^64f6p$ 242694.9 ($J = 3$)	9.30E + 07	2.48E + 08	− 1.53
923.225	$5s^25p^64f^2$ 20050.6 ($J = 0$)	$5s^25p^64f5d$ 133366.3 ($J = 1$)^o	1.41E + 08	1.72E + 08	− 1.59
924.767	$5s^25p^64f5d$ 130553.0 ($J = 4$)^o	$5s^25p^64f6p$ 238688.0 ($J = 3$)	1.88E + 09	2.69E + 09	− 0.49
924.844	$5s^25p^64f5d$ 131104.7 ($J = 3$)^o	$5s^25p^64f6p$ 239232.5 ($J = 2$)	1.90E + 08	2.25E + 08	− 1.57
925.188	$5s^25p^64f5d$ 138275.4 ($J = 1$)^o	$5s^25p^64f6p$ 246362.2 ($J = 2$)	2.32E + 09	2.93E + 09	− 0.44
925.415	$5s^25p^64f5d$ 135027.2 ($J = 5$)^o	$5s^25p^64f6p$ 243087.0 ($J = 4$)	2.81E + 09	3.83E + 09	− 0.34
926.948	$5s^25p^64f^2$ 27478.7 ($J = 2$)	$5s^25p^64f5d$ 135359.2 ($J = 2$)^o	2.40E + 07	3.83E + 07	− 2.24
927.304	$5s^25p^64f^2$ 27478.7 ($J = 2$)	$5s^25p^64f5d$ 135318.3 ($J = 3$)^o	1.55E + 08	1.52E + 08	− 1.63
927.915	$5s^25p^64f5d$ 135318.3 ($J = 3$)^o	$5s^25p^64f6p$ 243087.0 ($J = 4$)	1.55E + 09	2.06E + 09	− 0.60
930.460	$5s^25p^64f^2$ 25892.9 ($J = 1$)	$5s^25p^64f5d$ 133366.3 ($J = 1$)^o	3.90E + 07	5.62E + 07	− 2.07
931.296	$5s^25p^64f5d$ 135318.3 ($J = 3$)^o	$5s^25p^64f6p$ 242694.9 ($J = 3$)	2.90E + 09	2.66E + 09	− 0.49
931.653	$5s^25p^64f5d$ 135359.2 ($J = 2$)^o	$5s^25p^64f6p$ 242694.9 ($J = 3$)	4.13E + 09	4.79E + 09	− 0.23
934.508	$5s^25p^64f5d$ 142910.8 ($J = 5$)^o	$5s^25p^64f6p$ 249919.6 ($J = 4$)	1.19E + 10	1.53E + 10	0.28
934.508	$5s^25p^64f^2$ 20551.4 ($J = 2$)	$5s^25p^64f5d$ 127558.8 ($J = 2$)^o	1.40E + 08	1.22E + 08	− 1.73
936.233	$5s^25p^64f5d$ 139549.8 ($J = 3$)^o	$5s^25p^64f6p$ 246362.2 ($J = 2$)	7.70E + 07	4.40E + 07	− 2.26
941.772	$5s^25p^64f5d$ 140180.8 ($J = 2$)^o	$5s^25p^64f6p$ 246362.2 ($J = 2$)	4.57E + 08	4.62E + 08	− 1.22
944.586	$5s^25p^64f5d$ 133366.3 ($J = 1$)^o	$5s^25p^64f6p$ 239232.5 ($J = 2$)	2.59E + 09	2.85E + 09	− 0.44
961.891	$5s^25p^64f5d$ 147601.4 ($J = 1$)^o	$5s^25p^64f6p$ 251563.0 ($J = 2$)	3.88E + 09	4.95E + 09	− 0.18
963.694	$5s^25p^64f5d$ 142910.8 ($J = 5$)^o	$5s^25p^64f6p$ 246677.6 ($J = 4$)	2.71E + 09	3.01E + 09	− 0.39
975.470	$5s^25p^64f5d$ 140180.8 ($J = 2$)^o	$5s^25p^64f6p$ 242694.9 ($J = 3$)	9.51E + 08	7.96E + 08	− 0.96
998.232	$5s^25p^64f5d$ 142910.8 ($J = 5$)^o	$5s^25p^64f6p$ 243087.0 ($J = 4$)	1.78E + 09	3.01E + 09	− 0.39
1866.896	$5s^25p^64f6s$ 197997.9 ($J = 3$)^o	$5s^25p^64f6p$ 251563.0 ($J = 2$)	3.73E + 09	4.17E + 09	0.35
1868.031	$5s^25p^64f6s$ 193598.5 ($J = 2$)^o	$5s^25p^64f6p$ 247130.7 ($J = 1$)	2.50E + 09	2.47E + 09	0.12
1895.243	$5s^25p^64f6s$ 193598.5 ($J = 2$)^o	$5s^25p^64f6p$ 246362.2 ($J = 2$)	2.43E + 09	2.15E + 09	0.08
1899.414	$5s^25p^64f6s$ 194029.5 ($J = 3$)^o	$5s^25p^64f6p$ 246677.6 ($J = 4$)	4.76E + 09	6.83E + 09	0.58
1902.492	$5s^25p^64f6s$ 197452.8 ($J = 4$)^o	$5s^25p^64f6p$ 250015.7 ($J = 5$)	6.24E + 09	8.06E + 09	0.65
1905.966	$5s^25p^64f6s$ 197452.8 ($J = 4$)^o	$5s^25p^64f6p$ 249919.6 ($J = 4$)	1.88E + 09	2.07E + 09	0.07
1912.874	$5s^25p^64f6s$ 197452.8 ($J = 4$)^o	$5s^25p^64f6p$ 249730.1 ($J = 3$)	1.57E + 09	2.37E + 09	0.13
1925.978	$5s^25p^64f6s$ 197997.9 ($J = 3$)^o	$5s^25p^64f6p$ 249919.6 ($J = 4$)	3.78E + 09	4.51E + 09	0.42
1933.032	$5s^25p^64f6s$ 197997.9 ($J = 3$)^o	$5s^25p^64f6p$ 249730.1 ($J = 3$)	2.71E + 09	2.74E + 09	0.20
1938.394	$5s^25p^64f6s$ 193598.5 ($J = 2$)^o	$5s^25p^64f6p$ 245187.5 ($J = 3$)	2.79E + 09	2.41E + 08	− 0.83
1954.726	$5s^25p^64f6s$ 194029.5 ($J = 3$)^o	$5s^25p^64f6p$ 245187.5 ($J = 3$)	1.55E + 09	3.79E + 08	− 0.63
2030.842	$5s^25p^64f6s$ 197452.8 ($J = 4$)^o	$5s^25p^64f6p$ 246677.6 ($J = 4$)	2.94E + 08	3.37E + 08	− 0.66

Table 6 – *continued*

λ_{obs} (Å)[a]	Transition		gA (s^{-1})		log gf
	Lower level	Upper level	Previous[a]	HFR + CPOL[b]	HFR + CPOL[b]
2190.667	$5s^25p^64f6s$ 197452.8 ($J = 4$)^o	$5s^25p^64f6p$ 243097.0 ($J = 4$)	1.86E + 09	2.88E + 09	0.32
2190.667	$5s^25p^64f6s$ 193598.5 ($J = 2$)^o	$5s^25p^64f6p$ 239232.5 ($J = 2$)	1.02E + 09	1.27E + 09	− 0.04
2209.637	$5s^25p^64f6s$ 197452.8 ($J = 4$)^o	$5s^25p^64f6p$ 242694.9 ($J = 3$)	1.48E + 09	1.63E + 09	0.08
2211.551	$5s^25p^64f6s$ 194029.5 ($J = 3$)^o	$5s^25p^64f6p$ 239232.5 ($J = 2$)	1.08E + 09	1.27E + 09	− 0.04
2217.127	$5s^25p^64f6s$ 193598.5 ($J = 2$)^o	$5s^25p^64f6p$ 238688.0 ($J = 3$)	1.64E + 09	1.47E + 09	0.03
2217.127	$5s^25p^64f6s$ 197997.9 ($J = 3$)^o	$5s^25p^64f6p$ 243087.0 ($J = 4$)	1.63E + 09	1.73E + 08	− 0.98
2236.596	$5s^25p^64f6s$ 197997.9 ($J = 3$)^o	$5s^25p^64f6p$ 242694.9 ($J = 3$)	1.16E + 09	1.48E + 09	0.05
2238.515	$5s^25p^64f6s$ 194029.5 ($J = 3$)^o	$5s^25p^64f6p$ 238688.0 ($J = 3$)	1.25E + 09	2.16E + 09	0.20

[a]Meftah et al. (2008) and Delghiche et al. (2015).
[b]This work.

et al. (2015) ranged from −2 per cent to 11 per cent with an average of 6.7 per cent and a standard deviation of 3.5 per cent.

In each ion, the E1 line strengths, S, were calculated in the Babushkin gauge with photon frequencies $\omega = 0$ (i.e. in the non-relativistic limit) using our AMBIT models. These were determined for the observed E1 transitions reported in Kaufman & Sugar (1967) for Pr V and in Meftah et al. (2008) and Delghiche et al. (2015) for Nd V. As only forbidden lines were published in Bekker et al. (2019) for Pr X, the E1 transitions involving the first two lowest even configurations, i.e. ($5s^25p^2$, $5s^25p4f$) → ($5s^25p5d$, $5s5p^3$, $5s5p^24f$), were selected.

4 RADIATIVE PARAMETERS

As it was already the case in our recent works focused on La V–X and Ce V–X ions (Carvajal Gallego et al. 2022a, b), among the three theoretical methods used, the HFR+CPOL approach proved to be the most convenient to obtain radiative parameters for a very large number of transitions, which is a crucial point for opacity calculations. Therefore, this method was chosen as the main method for the study of Pr V-X, Nd V-X, and Pm V-X ions, with the MCDHF and AMBIT approaches serving as benchmarks for the HFR+CPOL calculations performed in selected ions. The HFR + CPOL transition probabilities and oscillator strengths obtained in the present work are listed for all the experimentally observed lines published so far for the Pr, Nd, Pm ions of interest in Tables 5 and 6. These latter data concerned only Pr V (Table 5) and Nd V (Table 6) and were reported by Kaufman & Sugar (1967), on one hand, and by Meftah et al. (2008) and Delghiche et al. (2015), on the other hand. In Table 6, we also give the gA-values obtained by Meftah et al. and Delghiche et al. for Nd V lines who used the HFR method of Cowan (1981) but with much more limited bases of interacting configurations than the one considered in our work. This is reflected in the agreement between the two sets of results which, while globally satisfactory, shows quite significant deviations for a number of transitions.

Other oscillator strengths were also published for a very small number of transitions in the ions considered in the present work. These are in good agreement (generally by a few per cent) with our results. For instance, in the case of Pr V, we found average deviations between our HFR + CPOL gf-values and previous theoretical data of 9 per cent, 8 per cent, 8 per cent, 14 per cent, and 6 per cent when comparing with the relativistic single-configuration Hartree–Fock calculations of Migdalek & Baylis (1979), the relativistic model potential approach of Migdalek & Wyrozunska (1987), the relativistic many-body perturbation calculations of Savukov et al. (2003), the Dirac–Fock computations of Zilitis (2014), and the relativistic Hartree–Fock calculations of Karaçoban & Dogan (2015), respectively. The log gf-values deduced from all these previous works are compared to those obtained in the present work in Table 5.

More interesting are the cross comparisons between our HFR+CPOL, MCDHF, and AMBIT calculations we made for a handful of selected ions. Such comparisons are illustrated in Figs 2 and 3 where the HFR + CPOL oscillator strengths are plotted against the results obtained with the two other methods. More precisely, in Fig. 2, the HFR + CPOL log gf-values are compared with those computed using the MCDHF method for transitions involving the ground configuration in Pr V, Pr X, Nd V, Nd VI, Pm VI, and Pm IX ions, while in Fig. 3, the same type of comparison is made with the data obtained using the AMBIT code for the Pr V, Pr X, and Nd V ions. In these cases, we noted an overall good agreement, the average relative differences between HFR+CPOL and MCDHF oscillator strengths being found to be within 25 per cent whereas the mean deviations between HFR + CPOL and AMBIT gf-values were found to be within 35 per cent. However, larger discrepancies between the three methods were observed for some specific transitions mostly characterized by computed line strengths affected by strong cancellation effects or by large disagreements between length (Babushkin) and velocity (Coulomb) formalisms. The influence of these effects on opacity calculations will be discussed in Section 6. Nevertheless, in the light of these comparisons, we can expect the oscillator strengths calculated in our work to be affected by uncertainties of the order of 30 per cent for the strongest lines (log $gf > -1$) and a factor of two for weaker lines.

5 OPACITY CALCULATIONS

Using the whole set of HFR + CPOL atomic data obtained in the present work, the bound-bound opacities were calculated for Pr V–X, Nd V–X, and Pm V–X ions. Only allowed electric dipole lines (E1) were considered in the calculations, weaker forbidden transitions, such as magnetic dipole (M1) and electric quadrupole (E2) transitions, having a negligible contribution to the opacity of early phase kilonovae. The method of calculation was exactly the same as the one employed in our recent works on La V–X and Ce V–X (Carvajal Gallego et al. 2022a, b) and described by Sobolev (1960), Karp et al. (1977), Eastman & Pinto (1993), and Kasen, Thomas & Nugent (2006). We solved the Saha equation to determine the temperatures corresponding to the maximum ionic abundances for each of the elements considered. For doing so, the partition functions of Pr, Nd, and Pm ions were computed using the whole set of energy levels obtained in our HFR + CPOL calculations, the number of which is given in Table 7. In the same table, the ionization potentials taken from the NIST database (Kramida et al.

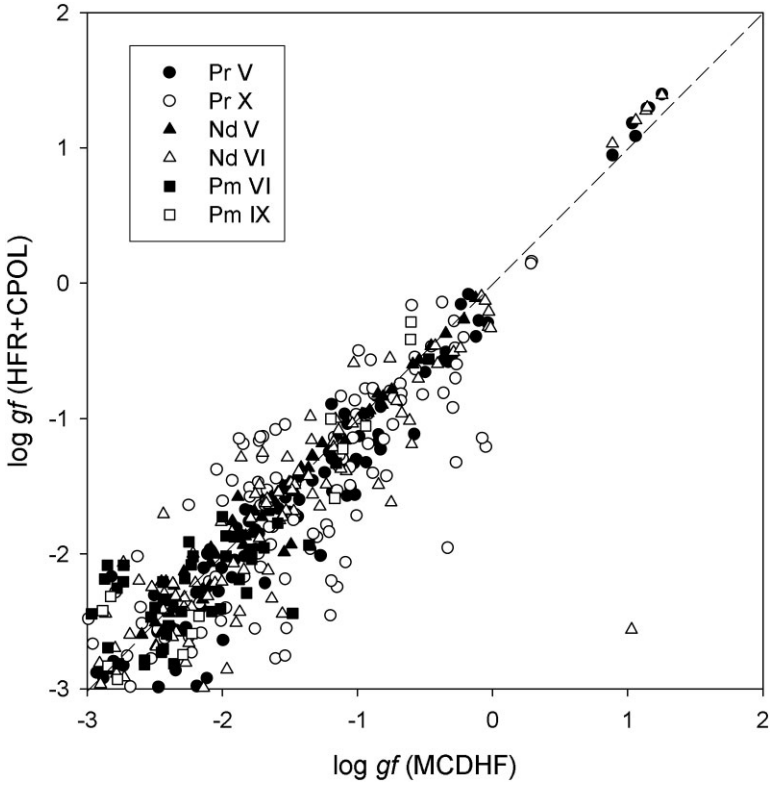

Figure 2. Comparison between the oscillator strengths (log *gf*) computed in this work using the HFR + CPOL and MCDHF methods for lines involving the ground-state configurations in Pr V, Pr X, Nd V, Nd VI, Pm VI, and Pm IX ions.

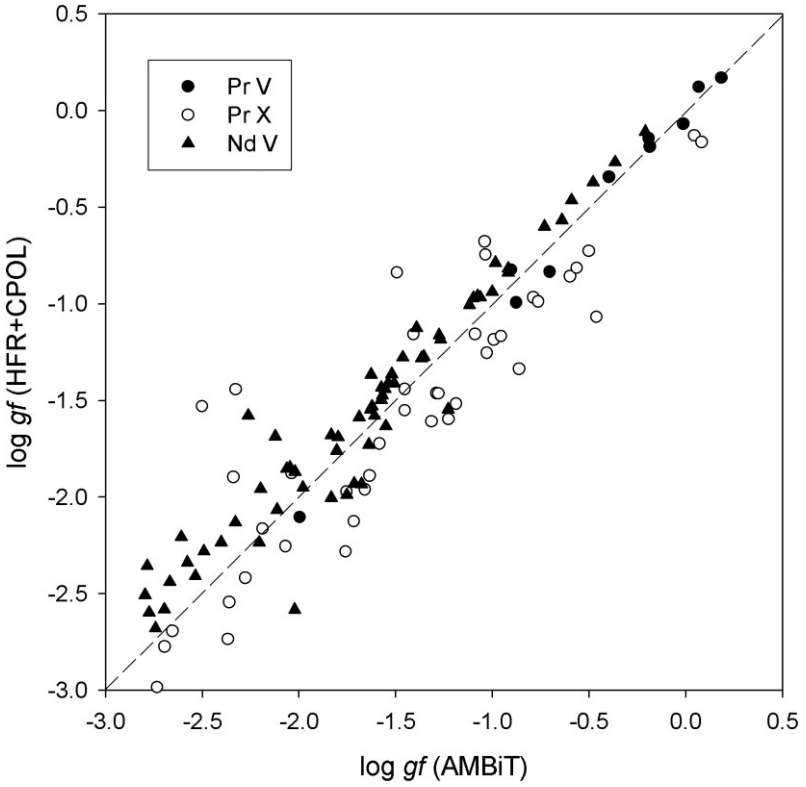

Figure 3. Comparison between the oscillator strengths (log *gf*) computed in this work using the HFR + CPOL and AMBIT methods for lines in Pr V, Pr X, and Nd V ions.

Table 7. Number of levels and transitions obtained in HFR + CPOL calculations and used for opacity determination in Pr V–X, Nd V–X, and Pm V–X. The ionization potentials and temperatures considered in opacity calculations are also given for each ion.

Ion	Levels[a]	Transitions[b]	IP (cm^{-1})[c]	T (K)[d]
Pr V	735	14 534	464 000	25 000
Pr VI	3447	203 360	663 000	33 000
Pr VII	7826	1017 797	784 000	40 000
Pr VIII	7694	1028 901	905 000	45 000
Pr IX	8298	1161 017	1060 000	55 000
Pr X	3974	865 860	1195 000	68 000
Nd V	2164	211 796	483 900	24 000
Nd VI	735	22 151	676 000	33 000
Nd VII	3447	497 534	799 000	40 000
Nd VIII	7826	1122 652	923 000	47 000
Nd IX	7694	1101 470	1093 000	56 000
Nd X	8298	1159 387	1224 000	65 000
Pm V	10 522	1152 223	497 900	24 000
Pm VI	3161	275 006	688 000	39 000
Pm VII	735	30 527	814 000	42 000
Pm VIII	3447	619 269	939 000	49 000
Pm IX	7826	1130 215	1116 000	58 000
Pm X	7694	1068 431	1250 000	67 000

[a]Total number of levels considered in HFR + CPOL calculations.
[b]Total number of transitions considered in opacity calculations (see text).
[c]Ionization potential taken from NIST (Kramida et al. 2022).
[d]Temperature deduced in the present work from the Saha equation and used in opacity calculations.

2022) and included in the calculations are also reported together with the deduced temperatures for all ions of interest.

The bound-bound opacities were then computed with these temperatures, considering a density $\rho = 10^{-10}$ g cm^{-3} and a time after merger $t = 0.1$ d, as suggested by Banerjee et al. (2020, 2022) for the early phases of kilonovae in which Pr V–X, Nd V–X, and Pm V–X are expected to be present. These conditions were assumed by the latter authors to be suitable for an ejecta mass $M_{ej} \sim 0.01$ $M_{\odot}$ and elements considered to be ionized up to $\sim$ XI therefore corresponding to typical temperatures given in Table 7.

The HFR + CPOL radiative parameters obtained for all transitions with log $gf > -5$ involving energy levels below the ionization potentials were included in the computations, as suggested by Fontes et al. (2020) and Carvajal Gallego et al. (2022a), giving rise to the final numbers of lines listed in Table 7. The expansion opacities thus obtained are plotted versus wavelengths in Figs 4, 5, and 6 for Pr V–X, Nd V–X, and Pm V–X, respectively.

6 IMPACT OF ATOMIC COMPUTATIONS ON THE OPACITIES

In this section, we examine the influence of some parameters related to the atomic calculations on the opacities.

In a first step, we studied the sensitivity of the opacities with respect to the arbitrarily chosen scaling factor in the HFR + CPOL calculations. As a reminder, in our work, all the Slater electrostatic interaction integrals (F^k, G^k, and R^k) were multiplied by a scaling factor of 0.90, as suggested by Cowan (1981), see Section 3.1. To examine the influence of this choice, we recalculated the opacities with atomic data from HFR + CPOL calculations in which we used 0.80, 0.85, and 0.95 as scaling factors. We found that the overall properties of opacities were not drastically affected by the choice of scaling factors (*SF*) in the atomic calculations, as illustrated in Fig. 7 where the Nd IX opacities obtained using HFR + CPOL atomic data with $SF = 0.80$, 0.85, 0.90, and 0.95 are compared.

A second effect evaluated was the one generated by the cancellation appearing when computing the oscillator strengths with the HFR + CPOL method. It was indeed found that most of transitions with log $gf < -2$ were affected by severe cancellation effects, which represents more than 75 per cent of the transitions calculated for the 18 ions considered in our work. As a reminder, such effects arise when the atomic states γJ and $\gamma' J'$ involved in a transition are strongly mixed because of intermediate coupling and configuration interaction. In this case, the wavefunctions are expanded in terms of basis functions,

$$|\gamma J >= \sum_{\beta} y^{\gamma}_{\beta J} |\beta J > \quad (3)$$

$$|\gamma' J' >= \sum_{\beta'} y^{\gamma'}_{\beta' J'} |\beta' J' > \quad (4)$$

and the line strength,

$$S = | < \gamma J || P^{(1)} || \gamma' J' > |^2 \quad (5)$$

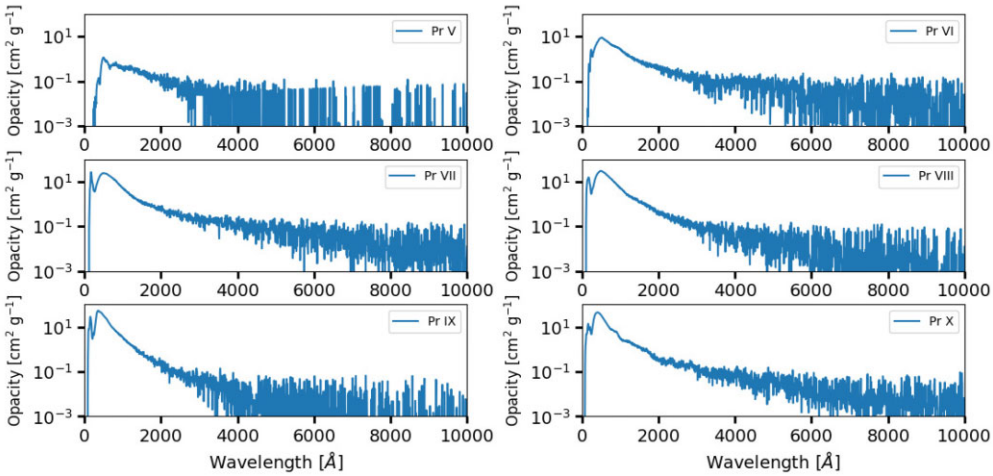

Figure 4. Expansion opacities for Pr V–X ions calculated with $\rho = 10^{-10}$ g cm^{-3}, $t = 0.1$ d, $\Delta\lambda = 10$ Å, and temperatures given in Table 7.

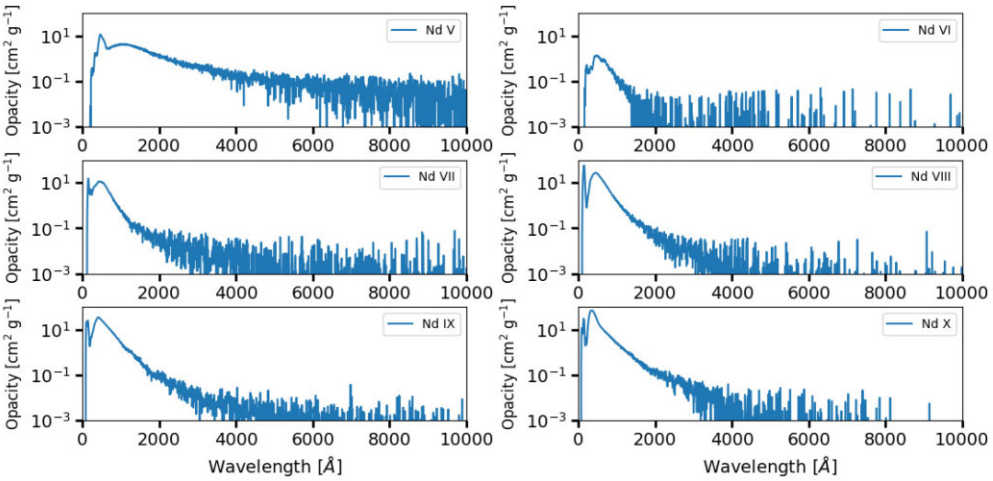

Figure 5. Expansion opacities for Nd V–X ions calculated with $\rho = 10^{-10}$ g cm^{-3}, $t = 0.1$ d, $\Delta\lambda = 10$ Å and temperatures given in Table 7.

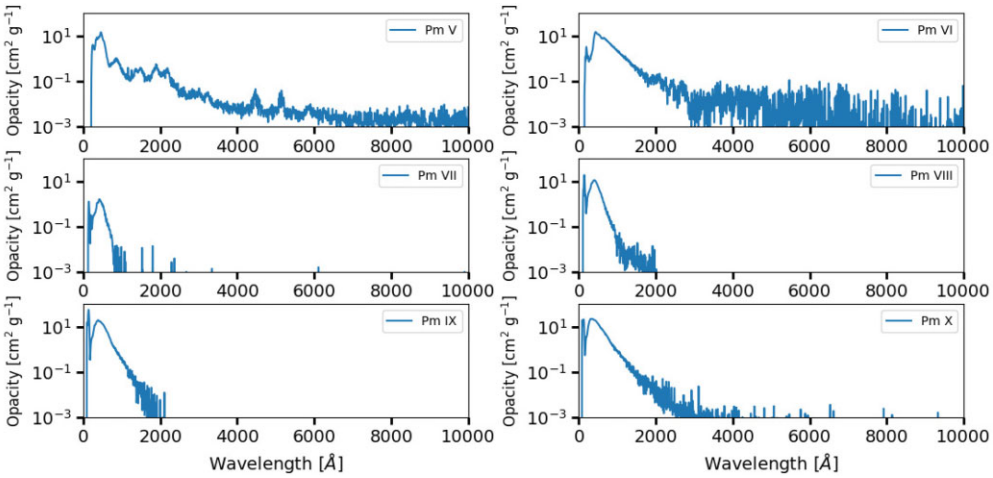

Figure 6. Expansion opacities for Pm V–X ions calculated with $\rho = 10^{-10}$ g cm^{-3}, $t = 0.1$ d, $\Delta\lambda = 10$ Å, and temperatures given in Table 7.

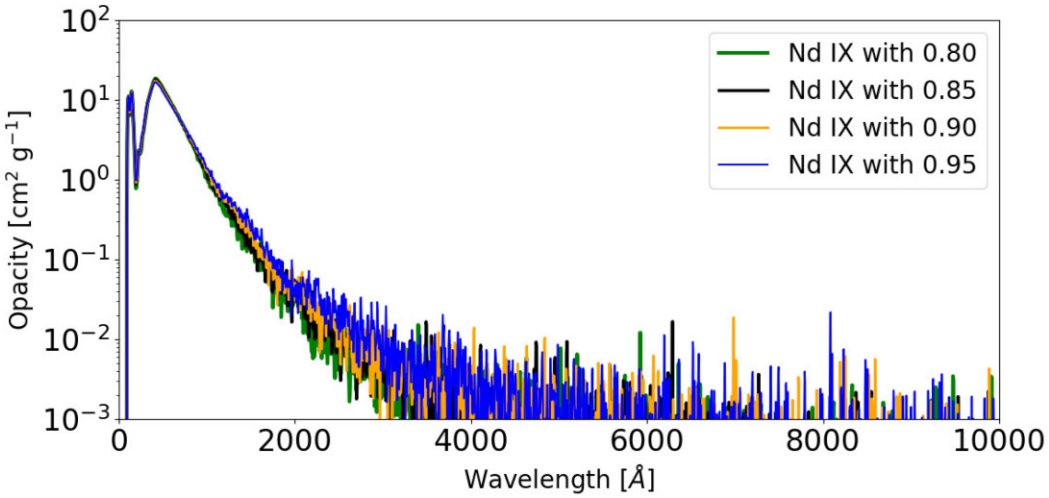

Figure 7. Comparison between opacities obtained for Nd IX using all HFR + CPOL transitions computed with electrostatic interaction parameters scaled down by a factor 0.80, 0.85, 0.90, and 0.95.

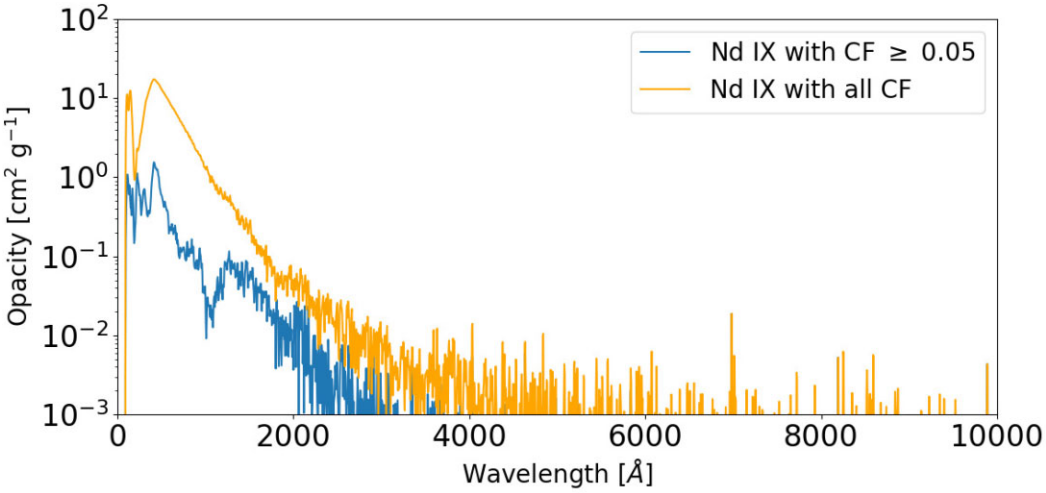

Figure 8. Comparison between opacities obtained for Nd IX using all transitions and those for which the CF are greater or equal to 0.05 in the HFR + CPOL calculations.

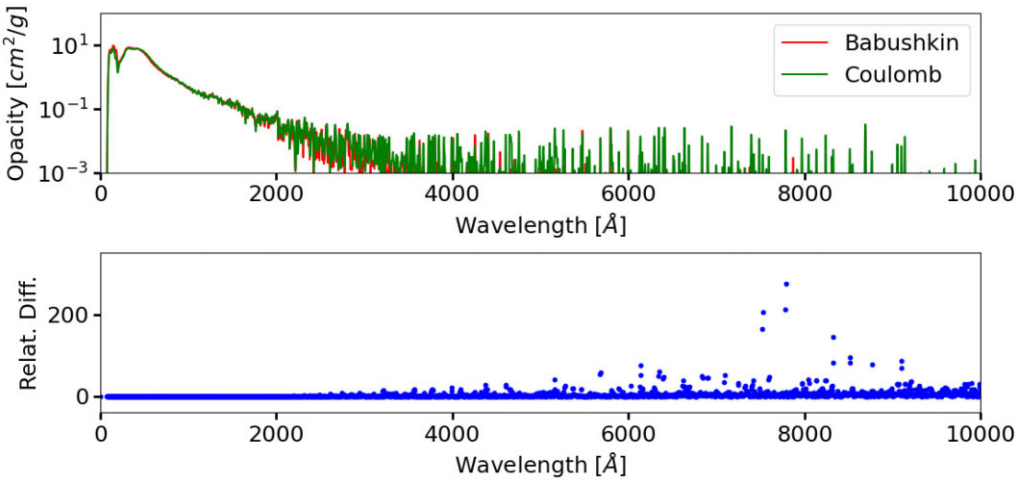

Figure 9. Comparison between opacities obtained for Nd IX using MCDHF transitions computed within the Babushkin and Coulomb gauges.

may be written in the form

$$S = |\sum_{\beta}\sum_{\beta'} y^{\gamma}_{\beta J} < \beta J||P^{(1)}||\beta' J' > y^{\gamma'}_{\beta' J'}|^2, \quad (6)$$

where $P^{(1)}$ is the dipole operator.

The sum appearing in the latter expression thus represents a mixing of amplitudes rather than line strengths themselves with the consequence that the effect of mixing is not necessarily a tendency to average out the various line strengths. There are frequently destructive interference effects that cause a weak line to become still weaker. In this context, the cancellation factor (CF) is given by

$$CF = \left[\frac{|\sum_{\beta}\sum_{\beta'} y^{\gamma}_{\beta J} < \beta J||P^{(1)}||\beta' J' > y^{\gamma'}_{\beta' J'}|}{\sum_{\beta}\sum_{\beta'} |y^{\gamma}_{\beta J} < \beta J||P^{(1)}||\beta' J' > y^{\gamma'}_{\beta' J'}|}\right]^2. \quad (7)$$

According to Cowan (1981), very small values of this factor (typically when CF is smaller than about 0.05) indicate that the corresponding transition rates should be taken with caution. Even if this type of effects affects only the weak transitions, the latter being very numerous in the calculations of opacities, we have analysed their influence on the whole spectral range considered in the present work. To do this, we compared the opacities obtained using all the transitions (with log $gf > -5$) calculated using the HFR + CPOL method with those deduced from transitions for which $CF \geq 0.05$. Such a comparison is shown in Fig. 8 in the case of Nd IX. As can be seen from this figure, the cancellation effects are distributed in a rather homogeneous way on the whole spectrum and thus do not seem to depend on the wavelength. Therefore, the consideration of the corresponding transitions in the opacity calculations does not have a dominant impact in a particular spectral region so that the uncertainties on the computed atomic transition rates due to strong cancellation effects are similarly distributed over the opacities throughout the whole spectrum.

Finally, as a number of MCDHF calculations were performed for a few selected ions in our work, it was interesting to investigate the influence of the Babushkin (length) or Coulomb (velocity) gauges used in the calculations of oscillator strengths. In Fig. 9, the Nd IX opacities obtained using the MCDHF radiative rates in both formalisms are compared. It is easy to see that the choice of the gauge has no significant influence on the deduced opacities, the relative difference between the two calculations exceeding a few per cent only in a few specific cases corresponding to very low opacities

at longer wavelengths. This simply reflects the large disagreements between the *gf*-values calculated within the Babushkin and Coulomb gauges for a handful of very weak transitions appearing at these wavelengths.

7 CONCLUSION

A new atomic data set was obtained for a large number of radiative transitions in Pr V–X, Nd V–X, and Pm V–X ions. A multiplatform approach using three independent theoretical methods, i.e. the pseudo-relativistic Hartree–Fock method including core-polarization effects (HFR+CPOL), the MCDHF approach and the Configuration Interaction Many-Body Perturbation Theory (CI + MBPT) allowed us to evaluate the accuracy of the oscillator strengths used for the determination of the opacities required for the analysis of the spectra emitted by kilonovae following neutron star mergers. A detailed study of the impact of atomic calculations on the opacities also showed that the computational strategy did not drastically alter the final results, as long as a sufficient number of radiative transitions were included in the opacity calculations.

ACKNOWLEDGEMENTS

HCG is holder of a FRIA fellowship while PP and PQ are, respectively, Research Associate and Research Director of the Belgian Fund for Scientific Research F.R.S.-FNRS. This project has received funding from the FWO and F.R.S.-FNRS under the Excellence of Science (EOS) programme (numbers O.0228.18 and O.0004.22). Part of the atomic calculations were made with computational resources provided by the Consortium des Équipements de Calcul Intensif (CECI), funded by the F.R.S.-FNRS under Grant No. 2.5020.11 and by the Walloon Region of Belgium.

DATA AVAILABILITY

The data underlying this article will be shared on reasonable request to the corresponding author.

REFERENCES

Abbott B. P. et al., 2017a, Phys. Rev. Lett., 119, 161101
Abbott B. P. et al., 2017b, ApJ, 848, L13
Banerjee S., Tanaka M., Kato D., Gaigalas G., Kawaguchi K., Domoto N., 2022, ApJ, 934, 117
Banerjee S., Tanaka M., Kawaguchi K., Kato D., Gaigalas G., 2020, ApJS, 901, 29
Bekker H., Borschevsky A., Harman Z., Keitel C. H., Pfeifer T., Schmidt P. O., Crespo Lopez-Urrutia J. R., Berengut J. C., 2019, Nat. Commun., 10, 5651
Berengut J. C., , Flambaum V. V., Kozlov M. G., 2006 , Phys. Rev. A, 73, 012504
Carvajal Gallego H., Berengut J. C., Palmeri P., Quinet P., 2022a, MNRAS, 509, 6138
Carvajal Gallego H., Berengut J. C., Palmeri P., Quinet P., 2022b, MNRAS, 513, 2302
Carvajal Gallego H., Palmeri P., Quinet P., 2021, MNRAS, 501, 1440
Cheng K. T., Froese Fischer C., 1983, Phys. Rev. A, 28, 2811
Cowan R. D., 1981, The Theory of Atomic Structure and Spectra. California Univ. Press, Berkeley
Delghiche D., Meftah A., Wyart J.-F., Campion N., Blaess C., Tchang-Brillet W.-Ü. L., 2015, Phys. Scr., 90, 095402
Eastman R. G., Pinto P. A., 1993, ApJ, 412, 731
Fontes C. J., Fryer C. L., Hungerford A. L., Wollaeger R. T., Korobkin O., 2020, MNRAS, 493, 4143
Fraga S., Karwowski J., Saxena K. M. S., 1976, Handbook of Atomic Data. Elsevier, Amsterdam
Froese Fischer C., Gaigalas G., Jönsson P., Bieroń J., 2019, Comput. Phys. Commun., 237, 184
Froese Fischer C., Godefroid M., Brage T., Jönsson P., Gaigalas G., 2016, J. Phys. B: At. Mol. Opt. Phys., 49, 182004
Gaigalas G., Kato D., Rynkun P., Radžiūtė L., Tanaka M., 2019, ApJS, 240, 29
Gaigalas G., Rynkun P., Radžiūtė L., Kato D., Tanaka M., Jönsson P., 2020, ApJS, 248, 13
Geddes A. J., Czapski D. A., Kahl E. V., Berengut J. C., 2018, Phys. Rev. A, 98, 042508
Glushkov A. V., 1992, J. Appl. Spectrosc., 56, 5
Grant I. P., 2007, Relativistic Quantum Theory of Atoms and Molecules. Springer, New York
Kahl E. V., Berengut J. C., 2019, Comput. Phys. Commun., 238, 232
Karaçoban U. B., Dogan S., 2015, Can. J. Phys., 93, 1439
Karp H., Lasher G., Chan K. L., Salpeter E. E., 1977, ApJ, 214, 161
Kasen D., Metzger B., Barnes J., Quataert E., Ramirez-Ruiz E., 2017, Nature, 551, 80
Kasen D., Thomas R. C., Nugent P., 2006, ApJ, 651, 366
Kaufman V., Sugar J., 1967, J. Res. Natl. Bur. Stand., 71A, 583
Kilbane D., O'Sullivan G., 2010, Phys. Rev. A, 82, 062504
Kramida A., Ralchenko Yu., Reader J., NIST ASD Team, 2022, NIST Atomic Spectra Database (ver.5.7.1.). Available online at https://physics.nist.gov/asd (accessed in July 2022)
Martin W. C., Zalubas R., Hagan L., 1978, Atomic Energy Levels - The Rare-Earth Elements, NSRDS-NBS 60. US Department of Commerce, Washington, DC
Meftah A., Wyart J.-F., Sinzelle J., Tchang-Brillet W.-Ü. L., Champion N., Spectro N., Sugar J., 2008, Phys. Scr., 77, 055302
Migdalek J., Baylis W. E., 1979, J. Quant. Spectrosc. Radiat. Transfer, 22, 127
Migdalek J., Wyrozumska M., 1987, J. Quant. Spectrosc. Radiat. Transfer, 37, 581
Quinet P., Palmeri P., Biémont E., Li Z. S., Zhang Z. G., Svanberg S., 2002, J. Alloys Comp., 344, 255
Quinet P., Palmeri P., Biémont E., McCurdy M. M., Rieger G., Pinnington E. H., Wickliffe M. E., Lawler J. E., 1999, MNRAS, 307, 934
Radžiūtė L., Gaigalas G., Kato D., Rynkun P., Tanaka M., 2020, ApJS, 248, 17
Radžiūtė L., Gaigalas G., Kato D., Rynkun P., Tanaka M., 2021, ApJS, 257, 29
Rynkun P., Banerjee S., Gaigalas G., Tanaka M., Radžiūtė L., Kato D., 2022, A&A, 658, A82
Savukov I. M., Johnson W. R., Safronova U. I., Safronova M. S., 2003, Phys. Rev. A, 67, 042504
Sobolev V. V., 1960, Moving Envelopes of Stars. Harvard Univ. Press, Cambridge
Stanek M., Migdalek J., 2004, J. Phys. B: At. Mol. Opt. Phys., 37, 2707
Tanaka M., Kato D., Gaigalas G., Kawaguchi K., 2020, MNRAS, 496, 1369
Zilitis V. A., 2014, Opt. Spectrosc., 117, 513

This paper has been typeset from a TEX/LATEX file prepared by the author.